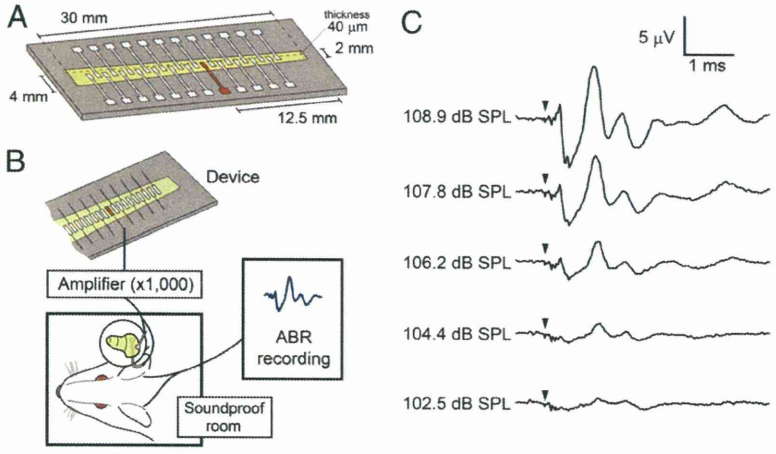


**Fig. 2.** ABR recording using a prototype device. (*A*) Schematic drawing of a prototype device with a piezoelectric membrane (yellow). A piezoelectric membrane has a thickness of 40 μm and a length of 30 mm. An array of 24 electrodes, made of aluminum thin film, is fabricated on the upper side of a piezoelectric membrane, which is aligned in the midline of the trapezoidal slit of the stainless plate. An electrode used in the experiment of stimulating auditory primary neurons is located 12.5 mm from the shorter side of the trapezoidal membrane (shown in red). (*B*) Schematic drawing of a setting for ABR recording using a piezoelectric device. Electrical signals generated by a piezoelectric membrane in response to acoustic stimuli are amplified and transferred to the cochlea. Bioelectrical signals were recorded as ABRs from needle electrodes inserted dorsal to ears. (*C*) ABRs by electrical signals derived from a prototype device by acoustic stimuli. Arrowheads indicate the timing of acoustic stimuli.

induced ABRs was almost similar to the latency between waves I and II of normal ABRs (0.83 ± 0.04 ms). These findings showed that the piezoelectric membrane generated biological ABRs by converting acoustic stimuli to electrical signals.

**Transmission of Sound Vibration from the External Auditory Canal to the Implanted Piezoelectric Device.** The transmission of sound waves from the external auditory canal to a piezoelectric membrane implanted into the cochlea is crucial to realize hearing recovery by a piezoelectric device based on the traveling wave theory. To test the transmission of sound waves from the external auditory canal to a piezoelectric membrane, we developed an implantable device that was specialized for the basal turn of the guinea pig cochlea (Fig. 3 *A* and *B*). The device contained a PVDF fluoride trifluoroethylene [P(VDF-TrFE)] membrane with a frequency response of 16–32 kHz, which corresponded to

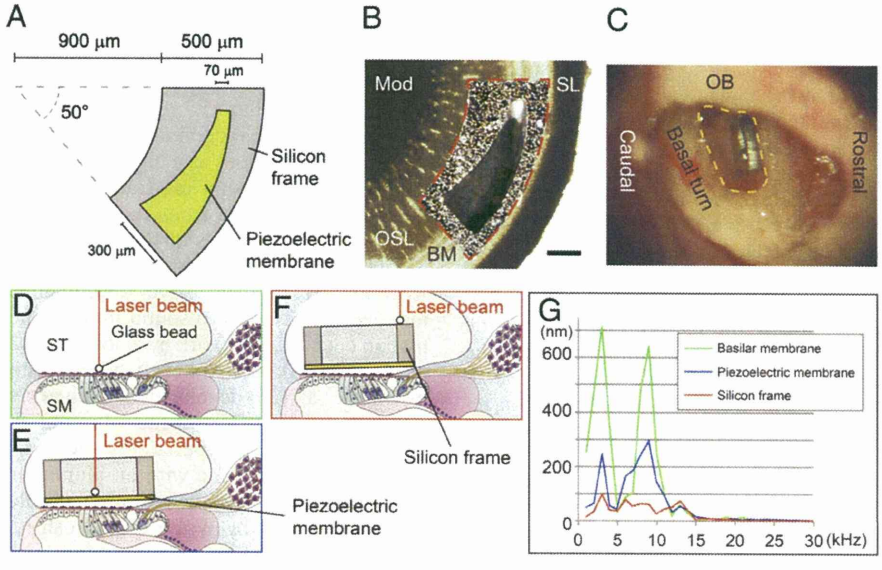


**Fig. 3.** Sound transmission from the external auditory canal to a piezoelectric device implanted in the cochlea. (*A*) Design of an implantable piezoelectric device. (*B*) A merged image of an implantable piezoelectric device and the basal turn of the guinea pig cochlea. To determine the radius of curvature of the outer border and the inner border of the fan-shaped silicon frame and location of the slit in the silicon frame, we measured radius of curvature of the cochlear basal turn, length between an inner edge of the spiral ligament (SL) and a medial end of the osseous lamina (OSL) where the device will be implanted, and length of the basilar membrane (BM; length between inner edge of spiral ligament and lateral end of osseous lamina). An outline of the silicon frame is shown by a red dotted line. The silicon frame is positioned on the osseous spiral lamina, and the slit of the device is located adjacent to the BM. Mod, cochlear modiolus. (Scale bar: 200 μm.) (*C*) A microscopic view of an implanted device in the basal turn of the guinea pig cochlea. The yellow dotted line indicates an opening in the basal turn of the cochlea. OB, otic bulla. (*D–F*) Schematic drawings of measuring vibration amplitudes using a laser Doppler vibrometer. A glass bead is placed on the BM (*D*), piezoelectric membrane (*E*), or silicon frame (*F*). Red lines indicate a laser beam from a laser Doppler vibrometer. SM, scala media; ST, scala tympani. (*G*) Vibration amplitudes of a BM (green), piezoelectric membrane (blue), and silicon frame (red) corresponding to frequencies of applied sounds.

the response of the basal turn of guinea pig cochleae (20). We implanted the device into the scala tympani of the basal portion of an intact cochlea (Fig. 3*C*). Before implantation, we measured the vibration of the basilar membrane in response to sound stimuli from the external auditory canal at various frequencies between 1 and 30 kHz. A glass bead (50-μm diameter) was placed on the basilar membrane (Fig. 3*D*), and its movement was measured using a laser Doppler vibrometer (21). When continuous pure tones were applied through the external auditory canal, the amplitudes for vibration of the basilar membrane showed peaks at 3 and 9 kHz (Fig. 3*G*, green line). In response to 3 kHz sound stimuli at 101.7 dB SPL, the largest amplitude was 642 nm, which was consistent with previous observations (21). Measurements of the vibratory movements of the piezoelectric membrane (Fig. 3*E*) also revealed two peaks of vibration amplitudes similar to the peaks of the basilar membrane (Fig. 3*G*, blue line). The maximum amplitude of the piezoelectric membrane was 293 nm in response to 9 kHz sound stimuli at 109.2 dB SPL.

In contrast to the piezoelectric membrane, measurements of the movements of the silicon frame (Fig. 3*F*) revealed no apparent peaks in the amplitudes of oscillations, which were all within 100 nm (Fig. 3*G*, red line). The differences in response between the piezoelectric membrane and silicon frame may be caused by the difference in the stiffness. In addition, the piezoelectric membrane was located closer to the basilar membrane than the silicon frame, and the basilar membrane may be a preferable location to receive sound vibration. These findings showed that sound stimuli transmitted through the external auditory canal caused vibration of a piezoelectric membrane implanted within the scala tympani of cochleae. Notably, the piezoelectric membrane exhibited similar tuning for sound frequency as the basilar membrane, indicating that it could reproduce the mechanical tonotopy of the latter. The tuning for sound frequency of the basilar and piezoelectric membranes differed from the tuning of the basilar membrane in normal guinea pig cochleae, which might have been caused by the opening of the cochlear wall for implantation of the device and taking measurements using a laser Doppler vibrometer.

**Generation of Voltage Output by the Implanted Device in Response to Sound Stimuli.** To show the technical feasibility of the piezoelectric hearing device, we examined whether sound stimuli generated electrical output from the piezoelectric membrane after implantation into the cochlea. For this purpose, we established an ex vivo model of a guinea pig temporal bone, in which sound stimuli were directly applied to the stapes, which transmits sound vibration to the oval window of the cochlea (Fig. 1 *A* and *B*). A miniaturized device modified to contain a silicon rod carrying electrodes for monitoring the voltage output from the piezoelectric membrane (Fig. 4 *A* and *B*) was implanted into the basal portion of cochleae. A miniaturized device was able to generate electrical output ranging from 0.14 to 5.88 mV in response to sound stimuli at 100 dB SPL at frequencies of 1–40 kHz in air (Fig. S3).

When 30-cycle tone-burst stimuli at 100 dB SPL at a frequency of 5, 10, or 20 kHz were directly applied to the stapes using an actuator, peak to peak voltage output of 23.7, 5.7, or 29.3 μV was recorded, respectively (Fig. 4*C*). After completion of the sound application, the amplitudes of voltage output gradually decreased and returned to the original level within 3 ms, which mimicked the biological response of the basilar membrane. In a control setting, in which an actuator generated sound stimuli but was not attached to the stapes, negligible voltage output was recorded (Fig. 4*C*). These findings showed that sound stimuli from the stapes generated voltage output from the piezoelectric device implanted in the cochlea. Notably, the voltage outputs from the piezoelectric device differed depending on the applied

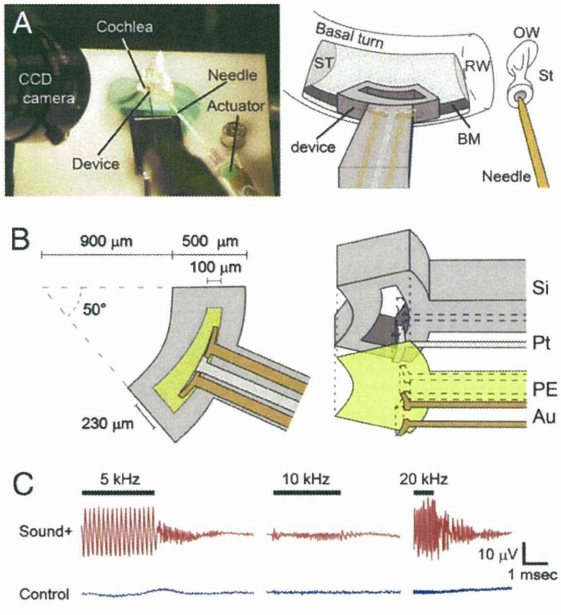


**Fig. 4.** Electrical output from the piezoelectric membrane implanted in the guinea pig cochlea in response to sound application to the stapes. (*A*) Photograph and schematic drawing showing the setting of an ex vivo system. A guinea pig temporal bone was set on a stage, and an implantable device was inserted into the scala tympani (ST) of the basal turn and placed close to the basilar membrane (BM). A needle was attached on the head of the stapes (St) to transmit sound vibrations through the oval window (OW). RW, round window. (*B*) Design of the implantable piezoelectric device. Au, gold film electrode; PE, piezoelectric membrane; Pt, platinum film electrode; Si, silicon frame. (*C*) Electrical output from a piezoelectric membrane in response to sound stimuli. Bars indicate the period for sound application. Waveforms in red show electrical output when sound stimuli are applied to the stapes, and waveforms in blue show those in a control setting.

sound frequency. The maximum voltage outputs in response to 5 and 20 kHz sound stimuli were similar (23.7 and 29.3 μV, respectively), whereas the outputs in response to 10 kHz sound stimuli were smaller (5.7 μV).

Researchers have previously attempted to develop an artificial cochlea that functions as a highly sophisticated sensor. Studies by von Békésy (4, 5) showing traveling waves in the basilar membrane using cochleae from cadavers led to the development of several physical models of the cochlea. The first group of these models comprised scaled-up versions of the cochlea (22–24). Recently, researchers have developed fluid-filled microscale models that respond to sound in a manner similar to the mammalian cochlea. The work by Zhou et al. (25) showed a tonotopic map over the 0.3- to 15-kHz band in a life-sized model. The work by Chen et al. (26) developed a beam array fixed on a trapezoidal channel and investigated the vibrating characteristics in water. The work by Wittbrodt et al. (27) developed a device containing a polyimide membrane with an aluminum frame, which shared some similarities with the biological cochlea in terms of traveling waves. The work by White and Grosh (28) used silicon micromachining technology to create their cochlea model. This work was important, because the batch micromachining process used to fabricate this system paved the way for the future integration of sensing elements into the structure to produce low-power, micromechanical, and cochlear-type sensor filters. However, these devices have no potential for generating electrical output in response to sound stimuli. Providing high-quality hearing through the cochlear implant involves the development of a device with high channel capability, low-power requirements, and small size (29). The work by Bachman et al. (29) fabricated

a micromechanical multiband transducer that consisted of an array of micromachined polymer resonators, and it examined its sensitivity to sound frequency; however, the work focused on the low-power requirements of the transducer and proposed a design that could be implanted into the middle ear cavity (29), which fundamentally differed from our concept.

The present report describes a device at the technology–biology interface that can mimic the function of the basilar membrane and inner hair cells using a combination of traditional traveling wave theory and microelectromechanical systems. This device could be described as the technological regeneration of hair cells. The device, which consists of a piezoelectric membrane and silicon frame, can be implanted into the guinea pig cochlea. It is able to resonate in response to sound stimuli similar to the natural basilar membrane and generate electric output, whereas previously reported devices required an electrical supply, and realizing low-energy requirements remains a goal for the future development of cochlear implants (29). We, therefore, consider the ability of our device to generate electrical output in response to sound stimuli to be a great advantage. In practice, the electrical output from our device is not sufficient to stimulate auditory primary neurons. The electrical output should be $10^5$-fold higher than the output of the present device for effective stimulation of auditory primary neurons when electrodes are placed in the scala tympani similar to conventional cochlear implants. We should optimize the location and fixation of a piezoelectric device in a cochlea for obtaining the maximum oscillation of a piezoelectric membrane, because electrical output from a piezoelectric membrane after implantation in a cochlea decreased to ~10% of electrical output recorded in the in vitro setting (Fig. S3). To increase the power of a piezoelectric device, we will examine the potential of other piezoelectric materials for generation of electrical output and the effects of reduction in thickness of a piezoelectric membrane and multilayer constructions of piezoelectric membranes. In addition, it is also important to reduce electrical output required for sufficient stimulation of auditory primary neurons. For this purpose, we are developing microelectrodes that are able to access close to auditory primary neurons. Finally, our device has only passive sensitivity to sound frequencies. To enhance this sensitivity, additional mechanisms mimicking the function of outer hair cells need to be developed.

## Materials and Methods

**Experimental Animals.** A total of 26 female adult Hartley guinea pigs (4–10 wk, 300–600 g in weight; Japan SLC) with a normal Preyer pinna reflex served as the experimental animals. Animal care was conducted under the supervision of the Institute of Laboratory Animals, Graduate School of Medicine, Kyoto University, Japan. All experimental procedures followed the National Institutes of Health Guidelines for the Care and Use of Laboratory Animals. In all procedures necessitating general anesthesia, the animals were administered an i.m. injection of midazolam (10 mg/kg; Astellas Pharma) and xylazine (0.01 mg/kg; Bayer). Supplemental doses were administered every 2 h or more often if the animal withdrew its leg in response to applied pressure.

**eABR Recording.** Measurements of eABRs were performed as previously described (30). Biphasic voltage pulses were generated under computer control using a real-time processor (Tucker-Davis Technologies). Electrical stimuli were applied between two intracochlear platinum–iridium electrodes. Bioelectrical signals were digitally amplified, averaged for 500 repetitions, and recorded using subdermal stainless steel needle electrodes.

**Prototype Piezoelectric Device.** The prototype piezoelectric device was fabricated as previously described (18). A thin aluminum film was formed on both sides of the 40-μm-thick PVDF membrane by sputtering. An electrode array with 24 rectangular elements was fabricated from the aluminum film using a standard photolithography and etching process on the upper side of the PVDF membrane. The aluminum film on the lower side served as a ground electrode.

**Prototype Device ABRs.** The ABRs produced using the prototype device were measured 7 d after the administration of KM and EA. The generation of trigger signals and the recordings of the evoked potentials were performed using PowerLab/4sp. The trigger signals were conveyed to a function generator (WF1945B; NF Corporation), which was programmed to generate a sinusoidal output signal for each trigger. The amplitudes and frequencies of the sinusoidal outputs were digitally controlled at a base frequency and duration of 5 kHz and 0.2 ms, respectively. The output signals were connected to a custom-made actuator, which delivered acoustic waves to the device. The amplitudes applied to the actuator were calibrated to produce vibrations of the piezoelectric membrane of the device equivalent to those vibrations produced by the application of sound at pressure levels ranging from 87 to 115 dB SPL. The electrical signals generated by the prototype device in response to the acoustic waves of the actuator were transmitted to a custom-made amplifier, which produced a 1,000-fold increase, and their waveforms and amplitudes were monitored by an oscilloscope (WaveJet 314A; LeCroy). A biphasic signal was extracted from the electrical signals using a custom-made complementary metal oxide semiconductor switch to prevent the signal induced by reverberation of the piezoelectric membrane. Signals from the complementary metal oxide semiconductor switch were also conducted to platinum–iridium electrodes implanted in the scala tympani of the cochlear basal turn of guinea pigs ($n$ = 4) placed in a soundproof room. The bioelectrical signals were averaged for 500 repetitions, and they were recorded using subdermal stainless steel needle electrodes. The responses were verified at least two times.

**Implantable Miniaturized Device.** An implantable device for examining the transmission of sound from the external auditory canal to the piezoelectric membrane was fabricated using a P(VDF-TrFE) membrane (KF-W#2200; Kureha) and a silicon frame according to the methods described previously (31). The surface of the 300-μm-thick silicon substrate (100) was penetrated by hexamethyldisilazane (Tokyo Ohka Kogyo) to enhance adhesion of the P(VDF-TrFE) membrane. An *N,N*-dimethylformamide (Nacalai Tesque) solution containing P(VDF-TrFE) at a concentration of 8% weight was spun on the silicon substrate. It was then heated to crystallize the P(VDF-TrFE) at a thickness of 3 μm. The opposite side of the silicon substrate was treated with photolithography and an etching process to form a fan-shaped silicon frame with a slit to accommodate the flexible piezoelectric membrane. The fan-shaped silicon frame and the location of the slit were designed based on the shape of the cochlear basal turn of adult guinea pigs. The slit in the silicon frame was positioned such that the sheet was adjacent to the portions of the basilar membrane where it vibrated the most (32).

**Surgical Procedure for Implantation of the Miniaturized Device into the Cochlea.** A laser Doppler vibrometer (LV-1100; Ono Sokki) was used to measure the vibrations of the basilar membrane and the piezoelectric membrane of the device implanted in the cochlea. Under general anesthesia, a retroauricular incision was made to expose the bulla of an experimental animal with a normal cochlea ($n$ = 1). An opening was made in the otic bulla while preserving the tympanic annulus, tympanic membrane, and ossicles. This opening was used to direct the laser beam to the cochlea to measure the vibrations. After a skin incision in the submandibular region, cochleostomy was made in the scala tympani of the basal turn for insertion of the implantable device. After a tracheotomy, suxamethonium chloride hydrate (10 mg; Kyorin Pharmaceutical) was injected i.m., and a ventilation tube was inserted into the trachea to suppress movements from spontaneous ventilation.

**Measurement of Vibrations Using a Laser Doppler Vibrometer.** Sine wave signals produced by a function generator were delivered to an electrostatic speaker driver (ED1; Tucker-Davis Technologies) to generate pure tones from an electrostatic speaker as acoustic stimuli. Continuous pure tones were applied through the external auditory canal of the animals from 1 to 30 kHz at 1-kHz intervals at levels between 62.5 and 109.2 dB SPL. We measured the vibrations in response to sound stimuli using a laser Doppler vibrometer (21, 33). Initially, a glass bead (50-μm diameter) was set on the basilar membrane. A laser Doppler vibrometer beam was directed to the glass bead (Fig. 3). The vibrations of the basilar membrane were measured five times for each frequency and averaged using a custom-made program. Subsequently, the miniaturized device was manually inserted into the scala tympani with its piezoelectric membrane adjacent to the basilar membrane. The laser beam was directed to a glass bead either placed on the surface of the piezoelectric membrane (Fig. 3) or fixed on the silicon frame (Fig. 3) of the implantable device for reflection to detect vibrations.

**Miniaturized Device for Voltage Output Recording.** The design of an implantable miniaturized device for vibration measurement was modified to record the voltage output from the piezoelectric membrane after implan-

tation into a cochlea. An implantable miniaturized device was connected to a silicon rod carrying electrodes for monitoring the voltage output from the piezoelectric membrane. Two thin (40-nm thickness) gold electrodes, which faced the basilar membrane of the cochlea, were formed by thermal deposition on the piezoelectric membrane. One thin (100-nm thickness) platinum electrode was formed by rf magnetron sputtering on the opposite side of the piezoelectric membrane for recording the output voltage.

**Recording Voltage Output from the Piezoelectric Membrane in Response to Sound Stimuli.** Two right temporal bones of guinea pigs were used. The bony wall of the otic bulla was removed to expose the basal portion of the cochleae and the incudostapedial joint. After separating the head of the stapes from the incus, the tympanic membrane, malleus, and incus were removed. Cochleostomy of the basal portion of cochleae was performed to access the scala tympani. The temporal bones were then fixed on a stage. The head of the stapes and an actuator (AE0203D04F; NEC/TOKIN) were connected with a needle. The position of the tip of the needle was monitored by a CCD camera during the recording. Tone-burst signals were delivered to an actuator using a function generator (NF Corporation). A modified miniaturized device was inserted into the scala tympani of the basal portion of the cochleae through the cochleostomy site, and it was attached to the piezoelectric membrane and the basilar membrane using a micromanipulator. The scala tympani was filled with 285 mM mannitol solution during the recording. The voltage outputs from the piezoelectric membrane were transmitted to a custom-made amplifier that produced a 1,000-fold increase, and their waveforms and amplitudes were monitored with an oscilloscope (WaveRunner 44MXi-A; LeCroy).

**ACKNOWLEDGMENTS.** The authors thank Shin-ichiro Kitajiri and Norio Yamamoto for technical contributions to histological analyses and Kozo Kumakawa, Yasushi Naito, and Harukazu Hiraumi for contributions to the development of surgical procedures. This study was supported by grants for Research on Sensory and Communicative Disorders from the Japanese Ministry of Health, Labor and Welfare (to J.I.).

1. Dallos P (1996) *The Cochlea*, eds Dallos P, Popper AN, Fay RR (Springer, New York), pp 1–43.
2. Sarpeshkar R, Lyon RF, Mead C (1998) A low-power wide-dynamic-range analog VLSI cochlea. *Analog Integr Circuits Signal Process* 16:245–274.
3. Slepecky NB (1996) *The Cochlea*, eds Dallos P, Popper AN, Fay RR (Springer, New York), pp 44–129.
4. von Békésy G (1960) *Experiments in Hearing*, ed Wever EG (McGraw-Hill, New York), pp 404–429.
5. von Békésy G (1970) Travelling waves as frequency analysers in the cochlea. *Nature* 225:1207–1209.
6. Patuzzi R (1996) *The Cochlea*, eds Dallos P, Popper AN, Fay RR (Springer, New York), pp 186–257.
7. Belyantseva IA, Adler HJ, Curi R, Frolenkov GI, Kachar B (2000) Expression and localization of prestin and the sugar transporter GLUT-5 during development of electromotility in cochlear outer hair cells. *J Neurosci* 20:RC116.
8. Davis H (1983) An active process in cochlear mechanics. *Hear Res* 9:79–90.
9. Evans BN, Dallos P (1993) Stereocilia displacement induced somatic motility of cochlear outer hair cells. *Proc Natl Acad Sci USA* 90:8347–8351.
10. Zheng J, et al. (2000) Prestin is the motor protein of cochlear outer hair cells. *Nature* 405:149–155.
11. Liberman MC, et al. (2002) Prestin is required for electromotility of the outer hair cell and for the cochlear amplifier. *Nature* 419:300–304.
12. LeMasurier M, Gillespie PG (2005) Hair-cell mechanotransduction and cochlear amplification. *Neuron* 48:403–415.
13. Liberman MC, Rosowski JJ, Lewis RF (2010) *Schuknecht's Pathology of the Ear*, eds Merchant SN, Nadol JB (People's Medical Publishing House-USA, Shelton, CT), 3rd Ed, pp 104–127.
14. Merchant SN (2010) *Schuknecht's Pathology of the Ear*, eds Merchant SN, Nadol JB (People's Medical Publishing House-USA, Shelton, CT), 3rd Ed, pp 631–663.
15. Diaz RC (2009) Inner ear protection and regeneration: A 'historical' perspective. *Curr Opin Otolaryngol Head Neck Surg* 17:363–372.
16. Oshima K, Suchert S, Blevins NH, Heller S (2010) Curing hearing loss: Patient expectations, health care practitioners, and basic science. *J Commun Disord* 43:311–318.
17. Zeng FG, Rebscher S, Harrison WV, Sun X, Feng H (2008) Cochlear implants: System design, integration and evaluation. *IEEE Rev Biomed Eng* 1:115–142.
18. Shintaku H, et al. (2010) Development of piezoelectric acoustic sensor with frequency selectivity for artificial cochlea. *Sens Actuators A* 158:183–192.
19. Yamane H, Marsh RR, Potsic WP (1981) Brain stem response evoked by electrical stimulation of the round window of the guinea pig. *Otolaryngol Head Neck Surg* 89: 117–124.
20. Viberg A, Canlon B (2004) The guide to plotting a cochleogram. *Hear Res* 197:1–10.
21. Wada H, Homma Y, Takahashi S, Takasaka T, Ohyama K (1996) *Proceedings of the International Symposium on Diversity in Auditory Mechanics*, eds Lewis ER, et al. (World Scientific, Teaneck, NJ), pp 284–290.
22. Helle R (1977) Investigation of the vibrational processes in the inner ear with the aid of hydromechanical models. *J Audiol Techn* 16:138–163.
23. Chadwick RS, Fourney ME, Neiswander P (1980) Modes and waves in a cochlear model. *Hear Res* 2:475–483.
24. Lechner TP (1993) A hydromechanical model of the cochlea with nonlinear feedback using PVF2 bending transducers. *Hear Res* 66:202–212.
25. Zhou G, Bintz L, Anderson DZ, Bright KE (1993) A life-sized physical model of the human cochlea with optical holographic readout. *J Acoust Soc Am* 93:1516–1523.
26. Chen F, et al. (2006) A hydromechanical biomimetic cochlea: Experiments and models. *J Acoust Soc Am* 119:394–405.
27. Wittbrodt MJ, Steele CR, Puria S (2006) Developing a physical model of the human cochlea using micro-fabrication methods. *Audiol Neurootol* 11:104–112.
28. White RD, Grosh K (2005) Microengineered hydromechanical cochlear model. *Proc Natl Acad Sci USA* 102:1296–1301.
29. Bachman M, Zeng FG, Xu T, Li GP (2006) Micromechanical resonator array for an implantable bionic ear. *Audiol Neurootol* 11:95–103.
30. Ogita H, et al. (2009) Surgical invasiveness of cell transplantation into the guinea pig cochlear modiolus. *ORL J Otorhinolaryngol Relat Spec* 71:32–39.
31. Shintaku H, et al. (2010) Culturing neurons on MEMS fabricated P(VDF-TrFE) films for implantable artificial cochlea. *J Biomech Sci Eng* 5:229–235.
32. Nilsen KE, Russell IJ (1999) Timing of cochlear feedback: Spatial and temporal representation of a tone across the basilar membrane. *Nat Neurosci* 2:642–648.
33. Wada H, et al. (1999) Measurement of dynamic frequency characteristics of guinea pig middle ear by a laser Doppler velocimeter. *JSME Int J Ser C* 42:753–758.

Mutai et al. BMC Medical Genetics 2011, 12:135
http://www.biomedcentral.com/1471-2350/12/135

BMC Medical Genetics

RESEARCH ARTICLE Open Access

# Systematic analysis of mitochondrial genes associated with hearing loss in the Japanese population: dHPLC reveals a new candidate mutation

Hideki Mutai[1], Hiroko Kouike[1], Eiko Teruya[1], Ikuko Takahashi-Kodomari[1], Hiroki Kakishima[2], Hidenobu Taiji[3], Shin-ichi Usami[4], Torayuki Okuyama[2] and Tatsuo Matsunaga[1*]

## Abstract

**Background:** Variants of mitochondrial DNA (mtDNA) have been evaluated for their association with hearing loss. Although ethnic background affects the spectrum of mtDNA variants, systematic mutational analysis of mtDNA in Japanese patients with hearing loss has not been reported.

**Methods:** Using denaturing high-performance liquid chromatography combined with direct sequencing and cloning-sequencing, Japanese patients with prelingual (N = 54) or postlingual (N = 80) sensorineural hearing loss not having pathogenic mutations of m.1555A > G and m.3243A > G nor *GJB2* were subjected to mutational analysis of mtDNA genes (*12S rRNA*, $tRNA^{Leu(UUR)}$, $tRNA^{Ser(UCN)}$, $tRNA^{Lys}$, $tRNA^{His}$, $tRNA^{Ser(AGY)}$, and $tRNA^{Glu}$).

**Results:** We discovered 15 variants in *12S rRNA* and one homoplasmic m.7501A > G variant in $tRNA^{Ser(UCN)}$; no variants were detected in the other genes. Two criteria, namely the low frequency in the controls and the high conservation among animals, selected the m.904C > T and the m.1105T > C variants in *12S rRNA* as candidate pathogenic mutations. Alterations in the secondary structures of the two variant transcripts as well as that of m.7501A > G in $tRNA^{Ser(UCN)}$ were predicted.

**Conclusions:** The m.904C > T variant was found to be a new candidate mutation associated with hearing loss. The m.1105T > C variant is unlikely to be pathogenic. The pathogenicity of the homoplasmic m.7501T > A variant awaits further study.

## Background

Hearing loss manifests in more than 1 in 1000 persons at birth, and the frequency increases subsequently to 3 in 1000 by 4 years of age [1,2]. Approximately 50 to 70% of congenital and childhood deafness is estimated to be due to genetic mutations. In adults, the prevalence of hereditary hearing impairment has been estimated to be approximately 3.2 in 1000 [3]. Some of the mitochondrial DNA (mtDNA) genes, such as *12S rRNA*, $tRNA^{Leu(UUR)}$, and $tRNA^{Ser(UCN)}$, are known to be responsible for hereditary hearing loss [4]. Among them, the m.1555A > G mutation in *12S rRNA* is found relatively frequently (0.6-16%, depending on the ethnic group) in aminoglycoside-induced, congenital, and late-onset nonsyndromic hearing loss [4,5]. The m.1494C > T mutation in *12S rRNA* is also associated with aminoglycoside-induced and nonsyndromic hearing loss [6,7]. The m.3243A > G mutation in $tRNA^{Leu(UUR)}$ is associated with late-onset nonsyndromic hearing loss [8,9], maternally inherited diabetes and deafness (MIDD) [10,11], and mitochondrial myopathy, encephalopathy, lactic acidosis, stroke-like episodes (MELAS), which frequently presents with hearing loss [12,13]. The m.7445A > C/G/T [14-16], 7472insC [17], and 7510T > C mutations [18] in $tRNA^{Ser(UCN)}$ are also associated with

* Correspondence: matsunagatatsuo@kankakuki.go.jp
[1]Laboratory of Auditory Disorders, Division of Hearing and Balance Research, National Institute of Sensory Organs, National Tokyo Medical Center, Tokyo, Japan
Full list of author information is available at the end of the article

aminoglycoside-induced, nonsyndromic, or syndromic hearing loss.

In addition, many other variants in *12S rRNA* have been proposed to be associated with hearing loss [4]. Some variants such as m.827A > G [19,20], 961T > C [21], 961delT + Cn [21,22], 1005T > C [22], and 1095T > C in *12S rRNA* [22-26] are not definitively related to hearing loss, because they have been found in subjects with normal hearing and/or are not conserved among mammals [19,27-30]. Moreover, a variety of mitochondrial haplogroups often localize in specific ethnic groups, making it difficult to determine whether the mtDNA variants are associated directly with diseases, indirectly as risk factors, or simply with rare subhaplogroups [31-34]. Accumulating reports of various novel mtDNA mutations associated with hearing loss prompted us to evaluate these variants in patients with hearing loss in Japan, where mtDNA mutation studies have focused on a few limited nucleotide positions [35,36].

A single cell contains hundreds of mitochondria, and the mtDNA in each mitochondrion is occasionally heterogeneous, a feature called heteroplasmy [37]. The proportion of pathogenic mutations of heteroplasmic mtDNA is considered to be one of the reasons for the wide range of severity of phenotypes seen in patients with mitochondrial-related diseases, such as those reported in the case of the m.3243A > G mutation [38-40]. Denaturing high-performance liquid chromatography (dHPLC) is a sensitive method to detect heteroplasmic mutations that can be overlooked by simple direct sequencing and comparison of the scanned peaks or restriction fragment length polymorphism-PCR [28,41]. In this study, we conducted a systematic mutational analysis of mtDNA by dHPLC combined with direct sequencing and cloning-sequencing in samples from Japanese patients with hearing loss.

## Methods

### Subjects

Subjects with bilateral sensorineural hearing loss were recruited by the National Tokyo Medical Center and collaborating hospitals. Subjects' medical histories were obtained and physical examinations were performed to exclude those subjects with syndromic symptoms, diseases of the outer or/and middle ear, and environmental factors related to hearing loss such as history of infectious diseases, premature birth, and newborn meningitis. Patients with a history of use of ototoxic drugs were included in the study because these drugs are known to be associated with mitochondrial hearing loss. Prior to this study, the patients were confirmed not to have the m.1555A > G and m.3243A > G mutations or not to be diagnosed as having *GJB2* -caused hearing loss, as assessed by restriction fragment length polymorphism-PCR or together with direct sequencing if the heterozygotic 235delC mutation was detected in *GJB2* [42,43]. The 134 subjects were classified into prelingual hearing loss (onset before 5 years old, 20 males and 34 females) or postlingual hearing loss (onset at 5 years old or later, 31 males and 49 females) [1]. The control group consisted of 137 unrelated Japanese individuals with normal hearing as examined by pure-tone audiometry. All subjects or their parents gave prior informed consent for participation in this study. This study was approved by the ethics committee of National Tokyo Medical Center.

### Screening for mtDNA mutations by dHPLC

DNA was extracted from blood samples using the Gentra Puregene DNA isolation kit (QIAGEN, Hamburg, Germany). Initially, whole mtDNA from each patient was amplified in three overlapping fragments (1351-8197, 6058-12770, and 11706-2258) [44] by LATaq DNA polymerase (TaKaRa BIO, Shiga, Japan). PCR was conducted at 94°C for 1 min followed by 30 cycles of 98°C for 10 s and 68°C for 6.5 min. Then, using the PCR products as templates, variants were analyzed by the Mitoscreen assay kit (Transgenomic, Glasgow, UK). We amplified the genes *12S rRNA*, $tRNA^{Leu(UUR)}$, $tRNA^{Ser(UCN)}$, $tRNA^{Lys}$, $tRNA^{His}$, $tRNA^{Ser(AGY)}$, and $tRNA^{Glu}$, for which mutations were reported to be associated with hearing loss on the Hereditary Hearing Loss Homepage [45] when the study was started. The PCR products using primer sets MT4 (for *12S rRNA*), MT6 ($tRNA^{Leu(UUR)}$), MT10 ($tRNA^{Ser(UCN)}$), MT11 ($tRNA^{Lys}$), MT15 ($tRNA^{His}$ and $tRNA^{Ser(AGY)}$), and MT18 ($tRNA^{Glu}$) were incubated with the appropriate restriction enzymes, incubated for heteroduplex formation either with reference PCR products to detect homoplasmy or with their own PCR products to detect heteroplasmy, then analyzed by dHPLC (WAVE system, Transgenomic) according to the manufacturer's protocols.

The reference mtDNA was derived from a Japanese individual with normal hearing. Sequencing of the entire reference mtDNA revealed 750A > G and 1438A > G polymorphisms, and the mtDNA sequence was otherwise comparable to the revised Cambridge Reference sequence (AC_000021) [46,47]).

### DNA sequencing

When homoplasmic or heteroplasmic variants were detected, the PCR product was subjected to direct sequencing by the BigDye Terminator ver. 3 cycle sequencing kit and ABI genetic analyzer 3730 (Life Technologies, Carlsbad, CA). To sequence *12S rRNA*, an additional nested PCR product (656-1,266) was amplified with primers F (5'-tggtcctagcctttctattagctctt-3') and R (5'-tggcggtatataggctgagca-3'). To sequence $tRNA^{Ser}$

$^{(UCN)}$, an additional nested PCR product (7,209-7,609) was amplified with primers F (5'-atgccccgacgttactcg-3') and R (5'- acctacttgcgctgcatgtg-3'). To determine the proportion of heteroplasmic 1005T > C variant in the *12S rRNA*, the nested PCR (656-1,266) product was cloned and sequenced. Nested PCR was carried out by replacing AmpliTaq Gold DNA polymerase with PrimeSTAR DNA polymerase, which has 3'-proofreading activity (TaKaRa BIO), followed by the Zero Blunt TOPO PCR cloning kit (Life Technologies). We sequenced 54 clones derived from the proband mtDNA and 24 clones derived from the mtDNA of each of five siblings. Sequencing data were analyzed by SeqScape ver2.6 (Life Technologies) and DNASIS Pro (Hitachisoft, Tokyo, Japan). The sequencing results for each patient were compared with the revised Cambridge Reference sequence to identify mtDNA variants. The uniqueness of each mutation was evaluated by comparison with the mtSNP database [48], MITOMAP [49], and the Uppsala mtDB database [50].

### Prediction of pathogenicity of mtDNA variants

The variants were evaluated based on double selection as proposed by Leveque and coworkers [51], with modification. Initially, we measured the frequencies of each variant found in the controls in our study (N = 137) and in the mtSNP database (N = 672, including: centenarians in Gifu, centenarians in Tokyo, type 2 diabetes mellitus patients (without or with vascular disorders), overweight young adult males, non-overweight young adult males, Parkinson's disease patients, and Alzheimer's disease patients in Japan). The variants with a frequency of more than 3% in one of the groups were considered as non-pathologic polymorphisms. We used a frequency threshold lower than that previously used (4%) [51] because the mtSNP database of Japanese individuals and the controls reflect the patient ethnic group background more closely than the mtDB and therefore requires a lower frequency threshold to exclude polymorphisms. The nucleotide conservation in each gene from human and 50 mammalian species was evaluated by ClustalW. The additional file lists the mammalian species and the accession numbers of the mtDNA (Additional File 1: Table S1). The variant frequencies in the mtDB were calculated to determine if the low variant frequencies measured in the controls reflect rare haplotypes in the Japanese population and are more common worldwide. All the variants were also analyzed with PhyloTree (mtDNA tree Build 10) [52] to search for previously characterized variants in haplogroups. Pathogenicity of the variants was also evaluated by predicting the secondary structures of the mitochondrial transcripts with or without the variant using Centroid Fold [53,54].

## Results

dHPLC screening and subsequent direct sequencing in the patients identified 12 homoplasmic or heteroplasmic variants in *12S rRNA* and 1 homoplasmic variant in $tRNA^{Ser(UCN)}$ (Table 1). In addition, the 3 homoplasmic variants, m.752C > T, 1009C > T, and 1107T > C in *12S rRNA* were detected in the controls by direct sequencing. All the patients and the controls appeared to have the non-pathogenic m.750A > G and 1438A > G variants, as previously noted [49]. No $tRNA^{Glu}$, $tRNA^{Leu(UUR)}$, $tRNA^{Lys}$, $tRNA^{His}$, or $tRNA^{Ser(AGY)}$ variants were detected. Table 1 lists the number of patients found with each variant, the frequencies of the variants in the controls and among Japanese individuals with various clinical conditions (mtSNP, N = 672), previous reports of the variants, and the frequencies of the variants in the mtDB. We evaluated two criteria, namely that the frequency of the variants be < 3% in both the controls and in the Japanese database (mtSNP) and that the variant nucleotide conserved by >50% among the 51 mammalian species we considered [51]; based on this analysis, two *12S rRNA* variants, m.904C > T and 1005T > C, were selected as candidate pathogenic mutations and subjected to further study. Although the homoplasmic m.7501T > A variant in $tRNA^{Ser(UCN)}$ did not meet the conservation criteria, it was also subjected to further study because several other $tRNA^{Ser(UCN)}$ mutations have been reported to be associated with hearing loss, whereas the m.7501T > A variant has not been studied for its pathogenicity.

A novel homoplasmic m.904C > T variant in the*12S rRNA* was found in a 46-year-old female patient (Figure 1A). She did not possess additional mtDNA pathogenic mutations and showed prelingual, progressive hearing loss with tinnitus. The patient was suspected of hearing impairment as early as 4 years old and was diagnosed with sensorineural hearing loss at age 11. The audiometric examination showed mild hearing loss at low frequencies and no response at 1 kHz and higher frequencies (Figure 1B). She had no response to an otoacoustic emission test, indicating dysfunction of the auditory outer hair cells. The patient had no history of treatment with ototoxic drugs and did not suffer from any other symptoms. The siblings also suffered from prelingual, severe hearing loss (with similar ages of onset and severity), but their parents had normal hearing (Figure 1A). The patient bore two children with normal hearing. DNA samples were not obtained from other family members. The secondary structure of the variant 12S rRNA predicted by Centroid Fold suggested that substitution of C > T (transcribed as U) at position 904 of the *12S rRNA* results in gross structural alteration of the transcript region that includes nucleotide positions 862 to 917, in addition to truncation of the

**Table 1 Mitochondrial DNA variants identified in this study**

| Gene | Mutation | Homo/ heteroplasmy | prelingual HL (N = 54) | Late-onset HL (N = 80) | Controls (N = 137) | freq in controls (%) | Japanese (N = 672)[a] | freq in Japanese (%) | conservation index[b] | Previous report[c] | mtDB[c] (N = 2704) | freq in mtDB (%) |
|---|---|---|---|---|---|---|---|---|---|---|---|---|
| *12S rRNA* | 663A > G | homoplasmy | 3 | 5 | 2 | **1.5** | 48 | 7.1 | **29/51** | yes | 86 | 3.2 |
| | 709G > A | homoplasmy | 7 | 7 | 12 | 8.8 | 125 | 18.6 | 19/51 | yes | 444 | 16.4 |
| | 750A > G | homoplasmy | 54 | 80 | 137 | 100.0 | no data | no data | **49/51** | yes | 2682 | 96.7 |
| | 752C > T | homoplasmy | 0 | 0 | 9 | 6.6 | 17 | 2.5 | 44/51 | yes | 20 | 0.7 |
| | 827A > G | homoplasmy | 4 | 3 | 3 | **2.2** | 25 | 3.7 | **48/51** | yes | 54 | **2.0** |
| | **904C > T** | homoplasmy | 1 | 0 | 0 | **0.0** | 0 | **0.0** | **48/51** | none | 0 | **0.0** |
| | 961insC | homoplasmy | 1 | 0 | 3 | **2.2** | 1 | **0.1** | 9/51 | yes | 37 | **2.0** |
| | 961delT+ Cn | both | 0 | 1 | 4(2)[d] | **2.9** | no data | no data | 9/51 | yes | no data | no data |
| | **1005T > C** | both | 1 | 1(1) | 1 | **0.7** | 1 | **0.1** | **33/51** | yes | 7 | **0.3** |
| | 1009C > T | homoplasmy | 0 | 0 | 1 | 0.7 | 1 | 0.1 | 9/51 | yes | 2 | 0.1 |
| | 1041A > G | homoplasmy | 0 | 4 | 5 | 3.6 | 11 | **1.6** | **26/51** | yes | 14 | **0.5** |
| | 1107T > C | homoplasmy | 0 | 0 | 6 | 4.4 | 29 | 4.3 | 30/51 | yes | 34 | 1.26 |
| | 1119T > C | homoplasmy | 1 | 2 | 7 | 5.1 | 20 | 3.0 | 20/51 | yes | 26 | 1.0 |
| | 1382A > C | homoplasmy | 0 | 1 | 11 | 8.0 | 62 | 9.2 | **38/51** | yes | 65 | **2.4** |
| | 1438A > G | homoplasmy | 54 | 80 | 137 | 100.0 | 662 | 98.5 | **46/51** | yes | 2620 | 96.9 |
| *$tRNA^{Ser(UCN)}$* | 7501T > A | homoplasmy | 0 | 3 | 0 | **0.0** | 1 | **0.1** | 15/51 | yes | 1 | **0.0** |

Mitochondrial gene variants that met the criterion for association with hearing loss (HL) are underlined and in bold type. [a]Data from the mtSNP database [48]. [b]Based on the results of the multiple alignment by ClustalW. See Additional File 1: Table S1 for information on the species used to calculate the sequence conservation. [c]Uppsala mtDB database [50]. [d]Each number in parentheses indicates the number of individuals with a heteroplasmic variant.

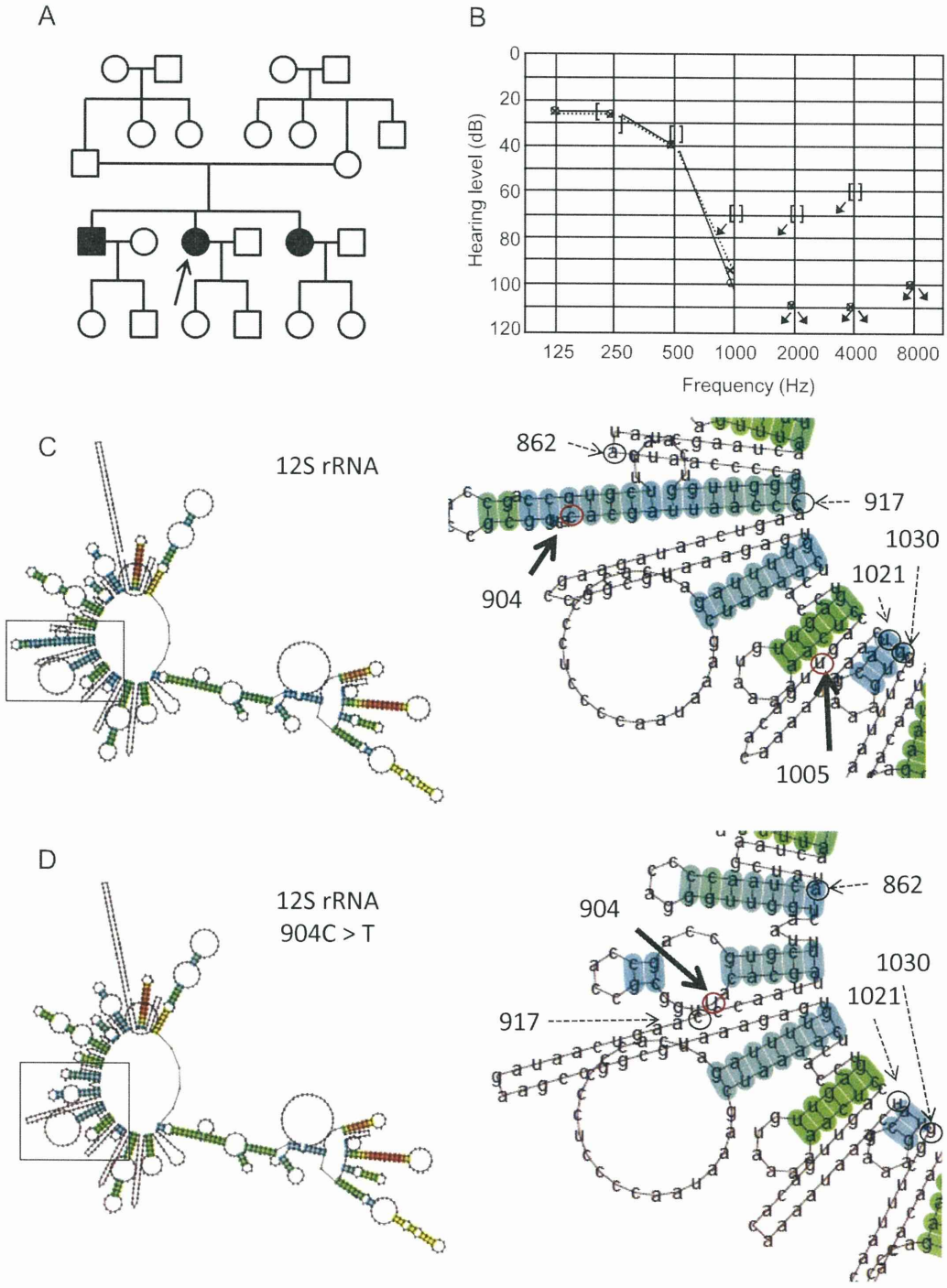


**Figure 1 Pedigree of a family carrying the m.904C > T variant**. (A) Pedigree of a family carrying the homoplasmic m.904C > T variant. Individuals with hearing loss are indicated by filled symbols. The arrow indicates the proband. (B) Audiogram of the proband of m.904C > T. Open circles with the line indicate the air conduction thresholds of the right ear; the X's with dotted line indicate the air conduction thresholds of the left ear; [, bone conduction thresholds of the right ear; ], bone conduction thresholds of the left ear. Arrows indicate the scale-out level of hearing loss. (C, D) Secondary structures of wild-type 12S rRNA (C) and 12S rRNA with the m.904C > T (D) predicted by Centroid Fold. To the right is shown an enlargement of the region of predicted secondary structures surrounding nucleotide positions including 904 and 1005 (bold arrows with red circles). Positions 862, 917, 1021, and 1030 are marked by dashed arrows with black circles for easy comparison of the structural changes. Each predicted base pair is indicated by a gradation of color (red to blue) corresponding to the base-pairing probability from 1 (red) to 0 (blue) according to Centroid Fold.

stem-like structure from positions 1021 to 1030 (Figure 1C and 1D), implicating a significant role for 904C in 12S rRNA folding.

The homoplasmic m.1005T > C variant in the *12S rRNA* was found in a male patient with prelingual, severe hearing loss (Figure 2A, B). The patient's spouse had prelingual hearing loss owing to measles, and their child also had prelingual hearing loss. The m.1005T > C variant was not detected in the patient's spouse or daughter. DNA samples were not obtained from other family members.

The heteroplasmic m.1005T > C variant together with the homoplasmic mutation m.709G > A was detected in a male patient from a consanguineous marriage of parents with normal hearing (Figure 2C). In the proband (III:3), onset of hearing loss and diabetes mellitus occurred in his 40s. Among his five siblings, four (III:1, 2, 4, 6) also showed adult-onset hearing loss between age 20 and 50 years, but they did not have diabetes mellitus. The fifth sibling suffered from infantile paralysis and died at age 6 (III:5). Cloning of the fragment of *12S rRNA*, which demonstrated apparent heteroduplex formation (Figure 2D, arrow), yielded 12 of 54 clones (22%) with the m.1005T > C variant. However, the m.1005T > C variant was not detected in 24 clones derived from the mtDNA from each of these siblings, indicating that the variant was absent in the siblings or the frequency was less than 4%. The audiograms showed severe to profound hearing loss in the siblings III:1, 2, 3, and 4 (Figure 2E, F, 3A, B). The secondary structure of the *12S rRNA* variant predicted by Centroid Fold indicated that the m.1005T > C induces a gross structural alteration in the transcript, including nucleotide positions 862 to 917 (Figure 1C and 3C).

Three patients appeared to carry the homoplasmic m.7501T > A variant in $tRNA^{Ser(UCN)}$ (Figure 4A, C, E). One female patient suffered from episodic vertigo from age 27 years followed by tinnitus and fluctuant, moderate progressive hearing loss, and she had no familial history of hearing loss (Figure 4A, B). Another female patient suffered from tinnitus beginning at age 24 years and had been exposed to streptomycin from age 36 to 37 for treatment of tuberculosis (Figure 4C, D). She suffered from fluctuant, moderate hearing loss from her 50s and had no familial history of hearing loss. The third patient was a male from a consanguineous marriage of parents with normal hearing and showed nonprogressive, severe hearing loss from childhood without tinnitus or vertigo (Figure 4E, F). Later, he was also found to have X-linked spinal and bulbar muscular atrophy (SBMA/Kennedy-Alter-Sung disease/Kennedy's disease). In this family, six of seven siblings showed hearing loss. Family members other than the proband did not participate in this study. According to the secondary structure prediction by Centroid Fold, the m.7501T > A in $tRNA^{Ser(UCN)}$ (which is transcribed as U in the reverse direction) causes an elongation of the D-arm in the transcript by reducing the size of the D-loop of $tRNA^{Ser(UCN)}$ (Figure 4G, H), which might affect biosynthesis of mitochondrial proteins [55].

## Discussion

In our study, screening of mtDNA by dHPLC and direct sequencing detected 15 variants in *12S rRNA* and 1 variant in $tRNA^{Ser(UCN)}$. Comparison of the variant frequencies in controls, assessment of nucleotide conservation among mammalian species, and structural analysis of the transcript was used to select candidate mutations associated with hearing loss. No variants in $tRNA^{Leu(UUR)}$, $tRNA^{Lys}$, $tRNA^{His}$, $tRNA^{Ser(AGY)}$, or $tRNA^{Glu}$ were detected in the subjects studied here, suggesting that the mutations in these genes associated with hearing loss are not common in the Japanese population.

To our knowledge, the homoplasmic m.904C > T variant in *12S rRNA* has not been reported elsewhere. Lack of symptoms in the maternal relatives does not exclude mitochondrial transmission, because penetrance of *12S rRNA* mutations can be extremely low, as seen in the m.1555A > G associated with hearing loss [56]. Conservation of the nucleotides among mammals and gross alteration of the predicted secondary structure of the *12S rRNA* transcript suggest that the m.904C > T variant might affect auditory function by changing the efficiency with which mRNAs are transcribed to yield mitochondrial proteins.

A patient with the homoplasmic m.1005T > C variant in the *12S rRNA* had a child with prelingual hearing loss. The inheritance of hearing loss in the child is likely due to the transmission of an autosomal mutation, not mtDNA, from the male proband. Therefore, the data for this family may not provide unequivocal information about the pathogenicity of the m.1005T > C variant [4,22,27,30].

Identification of the heteroplasmic m.1005T > C variant in a patient with hearing loss is a novel finding, because this variant has been known only as homoplasmic [22,27,30,34]. We did not verify that the heteroplasmic m.1005T > C variant was correlated with hearing loss because four of five siblings of the proband had hearing loss without carrying the variant, whereas it might be associated with diabetes mellitus. However, it is difficult to exclude the possibility of association of the heteroplasmic variant detected in blood samples with mitochondrial diseases such as deafness. Frequencies of heteroplasmy of mtDNA vary considerably among tissues in the same individual (for instance, [37,57,58]). Therefore, it is possible that the frequency of the m.1005T > C variant in the inner ear cells of the

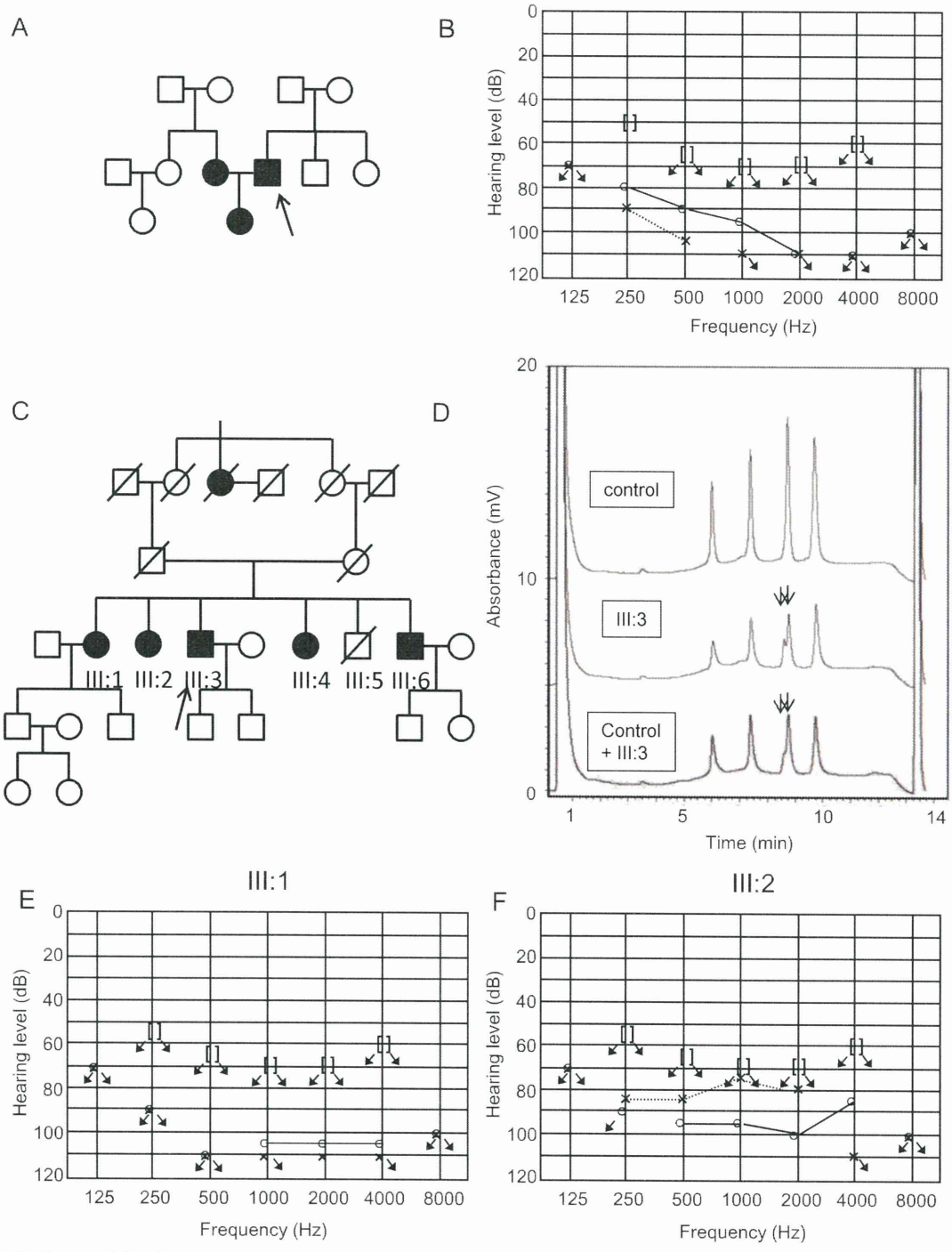


**Figure 2 Pedigrees of families carrying the m.1005T > C variant**. (A,B) Pedigree of a family carrying the homoplasmic m.1005T > C (A), and the audiogram of the proband (B). (C-F) Pedigree of a family carrying heteroplasmic m.1005T > C (C), and the chromatogram of dHPLC of the MT4 fragment of the proband (D). The arrows indicate split peaks of the fragment owing to the heteroplasmic m.1005T > C. Audiograms of the siblings (III:1, 2) are shown in (E-F).

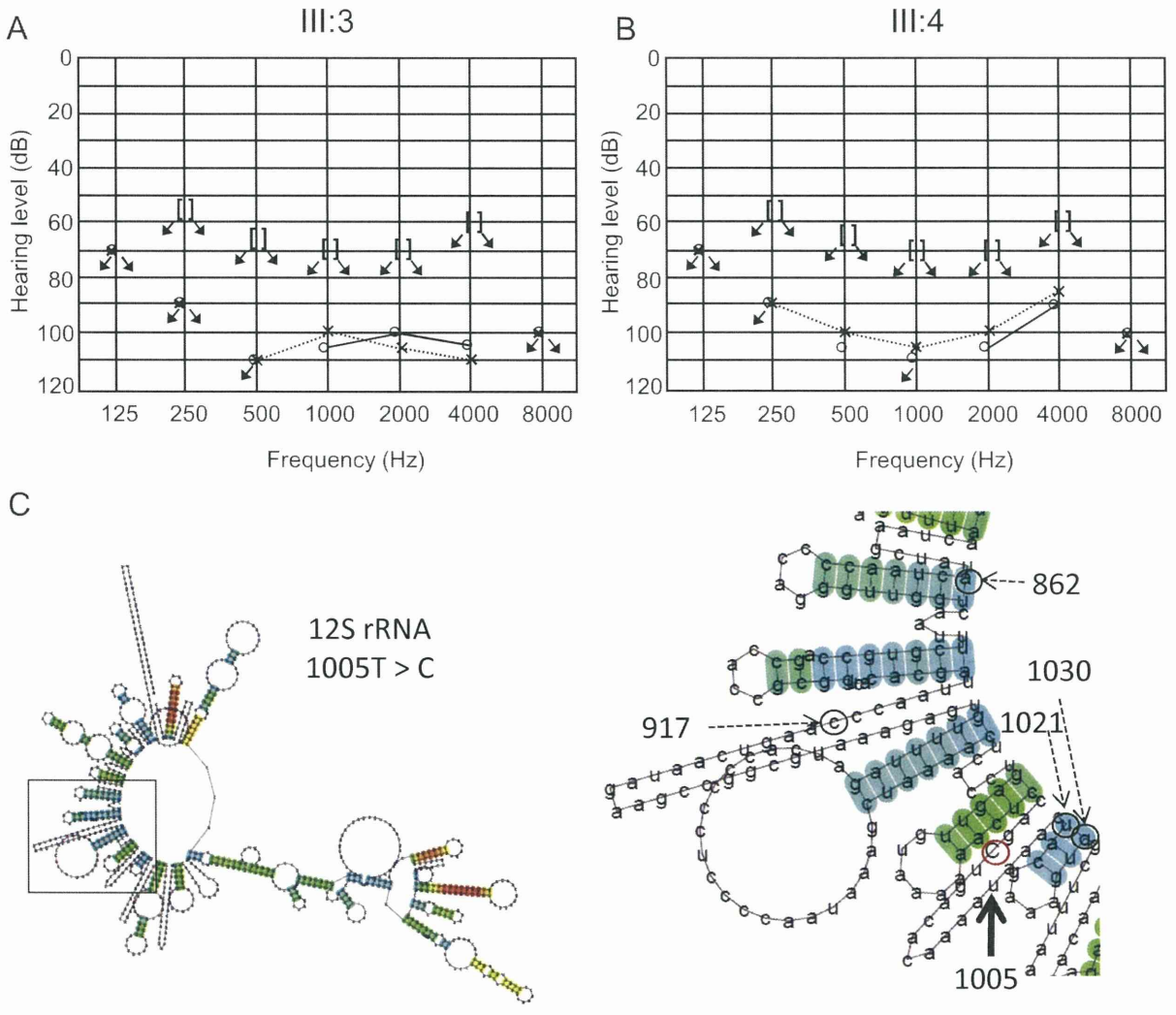


**Figure 3 Pedigrees of families carrying the m.1005T > C variant (continued)**. (A,B) Audiograms of the siblings (III: 3, 4) of a family carrying the heteroplasmic m.1005T > C (Figure 2C). (C) Predicted secondary structure of the *12S rRNA* transcript with the m.1005T > C. To the right is shown an enlargement of the region of predicted secondary structures surrounding nucleotide position 1005.

siblings is much higher than in the blood cells and thus may underlie the hearing loss.

Another finding in this study is that three patients with postlingual hearing loss had the homoplasmic m.7501T > A variant in $tRNA^{Ser\ (UCN)}$. Various mutations in $tRNA^{Ser(UCN)}$, such as m.7445A > G [15,16], 7472insC [17,59], 7505T > C [60], 7510T > C [18], and 7511T > C [51,59,61], are associated with various types of hearing loss (syndromic or nonsyndromic, prelingual or late-onset), raising the possibility that the m.7501T > A variant, reported elsewhere without detailed investigation [33], is also associated with hearing loss. The low conservation of the variation at this position (29% among mammals) does not support the pathogenicity of the variant, in contrast to the much higher conservation at m.7472A (61%), 7505A (98%), 7510T (78%), and 7511T (98%). On the other hand, the m.7501T > A variant is predicted to modify the secondary structure of the D-arm in the $tRNA^{Ser(UCN)}$ transcript; the D-arm is important for the stability of the transcript and the general rate of mitochondrial protein synthesis [55]. Further investigation, such as haplogroup analysis or generating lymphoblastoid cell lines to measure endogenous respiration rates, may help to define the pathogenicity of the m.7501T > A variant.

All other variants found in this study, such as m.827A > G, 961insC, and 961delT + Cn, which have been discussed elsewhere with respect to their pathogenicity [21,22,27,30,62], were considered to be non-pathologic polymorphisms because they were found frequently in

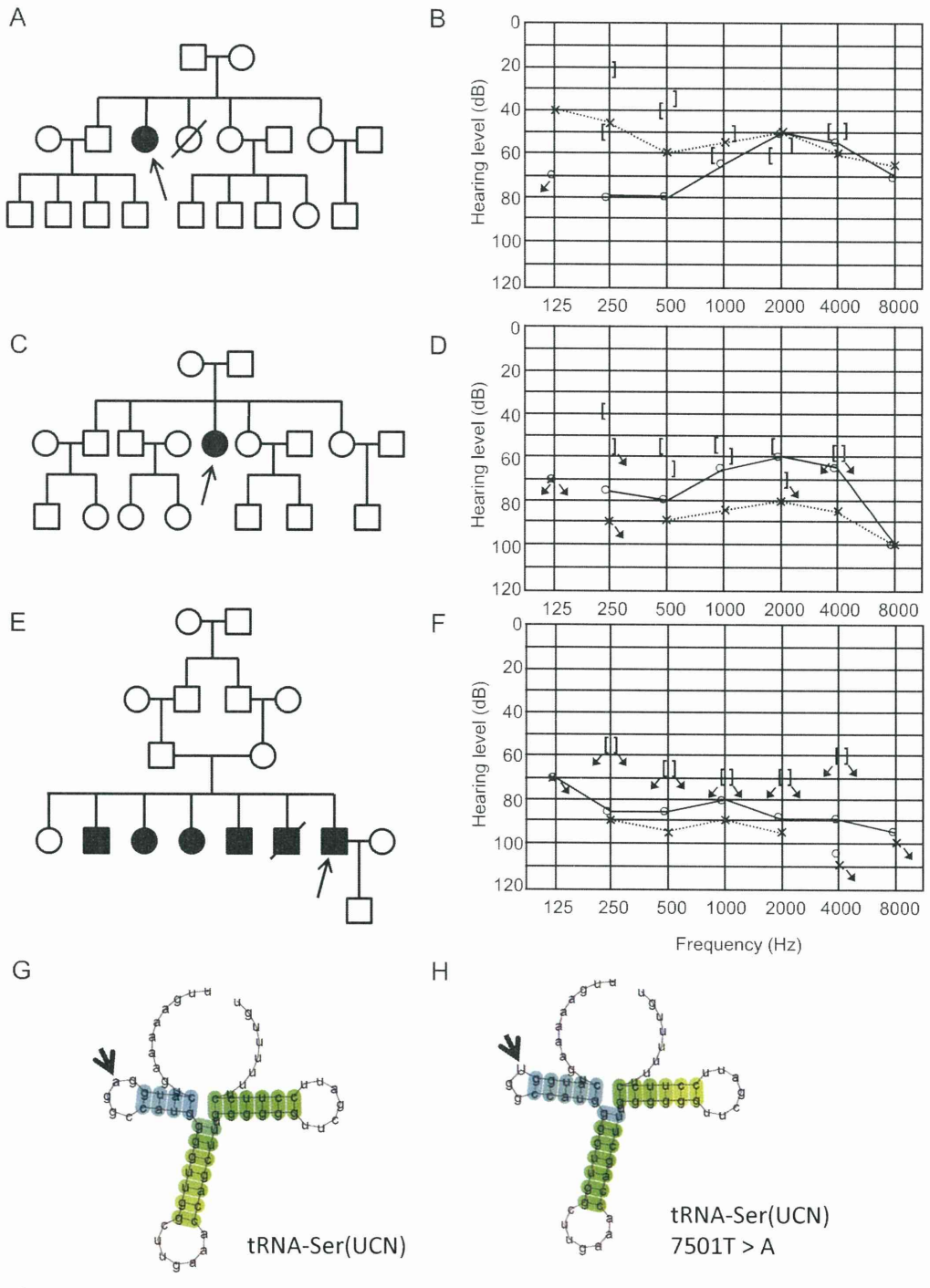


**Figure 4 Pedigrees of families carrying the m.7501T > A variant**. (A-F) Pedigrees of three families carrying the homoplasmic m.7501T > A, and audiograms of the probands (A and B, C and D, E and F). (G,H) Predicted secondary structure of the *tRNA*$^{Ser(UCN)}$ transcript (G) and the tRNA$^{Ser(UCN)}$ with m.7501T > A (H). Because the gene is transcribed in the reverse direction, thymine at 7501 (G) and adenine (H) are indicated as a and u, respectively (bold arrows).

the controls. The other variants, m.663A > G, 709G > A, 750A > G, 752C > T, 1009C > T, 1041A > G, 1107T > C, 1119T > C, 1382A > C, and 1438A > G, were frequently detected in the controls and considered to be nonpathogenic polymorphisms, which is in consistent with a previous report [27]. The spectrum of variants of mitochondrial genes in Japanese individuals was similar to that in a Chinese population [27], for which most of the variants detected in this study (other than the m.904C > T and 7501T > A) have been reported. In contrast, the spectrum was dissimilar to those in other ethnic groups such as the Polish population [19,63]. Our results indicate that ethnic background should be taken into consideration when studying the pathogenicity of mtDNA variants based on their frequencies in controls.

## Conclusions

We sought to detect mitochondrial variants other than m.1555A > G or 3243A > G mutations, which are known to be related to hearing loss, by dHPLC, direct sequencing, and cloning-sequencing in samples from Japanese patients with hearing loss. The homoplasmic m.904C > T variant in *12S rRNA* was considered to be a new candidate mutation associated with hearing loss. The pathogenicity of the m.7501T > A variant in $tRNA^{Ser(UCN)}$ remains inconclusive, and other variants identified in this study, including the heteroplasmic m.1005T > C variant, are not positively associated with hearing loss. No variants were detected in the in $tRNA^{Leu(UUR)}$, $tRNA^{Lys}$, $tRNA^{His}$, $tRNA^{Ser(AGY)}$, and $tRNA^{Glu}$.

## Additional material

**Additional file 1: Table S1.** List of animal species and the accession numbers of the mtDNA (GenBank) used to calculate nucleotide conservation.

### Acknowledgements and Funding

This study was supported by a Health Science Research Grant (H16-kankakuki-006 to TM) from the Ministry of Health, Labor, and Welfare of Japan, a Grant-in-Aid for Clinical Research to TM from the National Hospital Organization, and by a Grant-in-Aid for Scientific Research (19592001 to TM) from the Ministry of Education, Culture, Sports, Science and Technology of Japan.

### Author details

[1]Laboratory of Auditory Disorders, Division of Hearing and Balance Research, National Institute of Sensory Organs, National Tokyo Medical Center, Tokyo, Japan. [2]Department of Clinical Laboratory Medicine, National Center for Child Health and Development, Tokyo, Japan. [3]Division of Otorhinolaryngology, Department of Surgical Subspecialties, National Center for Child Health and Development, Tokyo, Japan. [4]Department of Otorhinolaryngology, Shinshu University School of Medicine, Nagano, Japan.

### Authors' contributions

HM participated in cloning and sequencing, data analysis, and drafted the manuscript. HKo, ET, ITK, and HKa established and conducted the dHPLC analysis, sequencing, and data analysis. HT, SU, and TO coordinated the study and helped with gene analysis. TM planned and organized the study, examined patients, analyzed data, and helped draft the manuscript. All the authors read and approved the final manuscript.

### Competing interests

The authors declare that they have no competing interests.

Received: 6 June 2011 Accepted: 12 October 2011
Published: 12 October 2011

### References

1. Morton CC, Nance WE: **Newborn hearing screening–a silent revolution.** *N Engl J Med* 2006, **354**:2151-2164.
2. Kral A, O'Donoghue GM: **Profound deafness in childhood.** *N Engl J Med* 2010, **363**:1438-1450.
3. Sakihara Y, Christensen B, Parving A: **Prevalence of hereditary hearing impairment in adults.** *Scand Audiol* 1999, **28**:39-46.
4. Kokotas H, Petersen MB, Willems PJ: **Mitochondrial deafness.** *Clin Genet* 2007, **71**:379-391.
5. del Castillo FJ, Rodriguez-Ballesteros M, Martin Y, Arellano B, Gallo-Teran J, Morales-Angulo C, Ramirez-Camacho R, Cruz Tapia M, Solanellas J, Martinez-Conde A, *et al*: **Heteroplasmy for the 1555A > G mutation in the mitochondrial 12S rRNA gene in six Spanish families with non-syndromic hearing loss.** *J Med Genet* 2003, **40**:632-636.
6. Chen J, Yang L, Yang A, Zhu Y, Zhao J, Sun D, Tao Z, Tang X, Wang J, Wang X, *et al*: **Maternally inherited aminoglycoside-induced and nonsyndromic hearing loss is associated with the 12S rRNA C1494T mutation in three Han Chinese pedigrees.** *Gene* 2007, **401**:4-11.
7. Zhao H, Li R, Wang Q, Yan Q, Deng JH, Han D, Bai Y, Young WY, Guan MX: **Maternally inherited aminoglycoside-induced and nonsyndromic deafness is associated with the novel C1494T mutation in the mitochondrial 12S rRNA gene in a large Chinese family.** *Am J Hum Genet* 2004, **74**:139-152.
8. Chinnery PF, Elliott C, Green GR, Rees A, Coulthard A, Turnbull DM, Griffiths TD: **The spectrum of hearing loss due to mitochondrial DNA defects.** *Brain* 2000, **123(Pt 1)**:82-92.
9. Deschauer M, Muller T, Wieser T, Schulte-Mattler W, Kornhuber M, Zierz S: **Hearing impairment is common in various phenotypes of the mitochondrial DNA A3243G mutation.** *Arch Neurol* 2001, **58**:1885-1888.
10. van den Ouweland JM, Lemkes HH, Ruitenbeek W, Sandkuijl LA, de Vijlder MF, Struyvenberg PA, van de Kamp JJ, Maassen JA: **Mutation in mitochondrial tRNA(Leu)(UUR) gene in a large pedigree with maternally transmitted type II diabetes mellitus and deafness.** *Nat Genet* 1992, **1**:368-371.
11. Maassen JA, Jahangir Tafrechi RS, Janssen GM, Raap AK, Lemkes HH, t Hart LM: **New insights in the molecular pathogenesis of the maternally inherited diabetes and deafness syndrome.** *Endocrinol Metab Clin North Am* 2006, **35**:385-396.
12. Goto Y, Nonaka I, Horai S: **A mutation in the tRNA(Leu)(UUR) gene associated with the MELAS subgroup of mitochondrial encephalomyopathies.** *Nature* 1990, **348**:651-653.
13. Kobayashi Y, Momoi MY, Tominaga K, Momoi T, Nihei K, Yanagisawa M, Kagawa Y, Ohta S: **A point mutation in the mitochondrial tRNA(Leu)(UUR) gene in MELAS (mitochondrial myopathy, encephalopathy, lactic acidosis and stroke-like episodes).** *Biochem Biophys Res Commun* 1990, **173**:816-822.
14. Jin L, Yang A, Zhu Y, Zhao J, Wang X, Yang L, Sun D, Tao Z, Tsushima A, Wu G, *et al*: **Mitochondrial tRNASer(UCN) gene is the hot spot for mutations associated with aminoglycoside-induced and non-syndromic hearing loss.** *Biochem Biophys Res Commun* 2007, **361**:133-139.
15. Reid FM, Vernham GA, Jacobs HT: **A novel mitochondrial point mutation in a maternal pedigree with sensorineural deafness.** *Hum Mutat* 1994, **3**:243-247.
16. Maasz A, Komlosi K, Hadzsiev K, Szabo Z, Willems PJ, Gerlinger I, Kosztolanyi G, Mehes K, Melegh B: **Phenotypic variants of the deafness-associated mitochondrial DNA A7445G mutation.** *Curr Med Chem* 2008, **15**:1257-1262.
17. Verhoeven K, Ensink RJ, Tiranti V, Huygen PL, Johnson DF, Schatteman I, Van Laer L, Verstreken M, Van de Heyning P, Fischel-Ghodsian N, *et al*: **Hearing impairment and neurological dysfunction associated with a**

mutation in the mitochondrial tRNASer(UCN) gene. *Eur J Hum Genet* 1999, 7:45-51.

18. Hutchin TP, Parker MJ, Young ID, Davis AC, Pulleyn LJ, Deeble J, Lench NJ, Markham AF, Mueller RF: **A novel mutation in the mitochondrial tRNA(Ser (UCN)) gene in a family with non-syndromic sensorineural hearing impairment.** *J Med Genet* 2000, **37**:692-694.
19. Rydzanicz M, Wrobel M, Pollak A, Gawecki W, Brauze D, Kostrzewska-Poczekaj M, Wojsyk-Banaszak I, Lechowicz U, Mueller-Malesinska M, Oldak M, *et al*: **Mutation analysis of mitochondrial 12S rRNA gene in Polish patients with non-syndromic and aminoglycoside-induced hearing loss.** *Biochem Biophys Res Commun* 2010, **395**:116-121.
20. Chaig MR, Zernotti ME, Soria NW, Romero OF, Romero MF, Gerez NM: **A mutation in mitochondrial 12S rRNA, A827G, in Argentinean family with hearing loss after aminoglycoside treatment.** *Biochem Biophys Res Commun* 2008, **368**:631-636.
21. Bacino C, Prezant TR, Bu X, Fournier P, Fischel-Ghodsian N: **Susceptibility mutations in the mitochondrial small ribosomal RNA gene in aminoglycoside induced deafness.** *Pharmacogenetics* 1995, **5**:165-172.
22. Li Z, Li R, Chen J, Liao Z, Zhu Y, Qian Y, Xiong S, Heman-Ackah S, Wu J, Choo DI, *et al*: **Mutational analysis of the mitochondrial 12S rRNA gene in Chinese pediatric subjects with aminoglycoside-induced and non-syndromic hearing loss.** *Hum Genet* 2005, **117**:9-15.
23. Thyagarajan D, Bressman S, Bruno C, Przedborski S, Shanske S, Lynch T, Fahn S, DiMauro S: **A novel mitochondrial 12SrRNA point mutation in parkinsonism, deafness, and neuropathy.** *Ann Neurol* 2000, **48**:730-736.
24. Tessa A, Giannotti A, Tieri L, Vilarinho L, Marotta G, Santorelli FM: **Maternally inherited deafness associated with a T1095C mutation in the mDNA.** *Eur J Hum Genet* 2001, **9**:147-149.
25. Wang Q, Li R, Zhao H, Peters JL, Liu Q, Yang L, Han D, Greinwald JH Jr, Young WY, Guan MX: **Clinical and molecular characterization of a Chinese patient with auditory neuropathy associated with mitochondrial 12S rRNA T1095C mutation.** *Am J Med Genet A* 2005, **133A**:27-30.
26. Zhao L, Young WY, Li R, Wang Q, Qian Y, Guan MX: **Clinical evaluation and sequence analysis of the complete mitochondrial genome of three Chinese patients with hearing impairment associated with the 12S rRNA T1095C mutation.** *Biochem Biophys Res Commun* 2004, **325**:1503-1508.
27. Lu J, Li Z, Zhu Y, Yang A, Li R, Zheng J, Cai Q, Peng G, Zheng W, Tang X, *et al*: **Mitochondrial 12S rRNA variants in 1642 Han Chinese pediatric subjects with aminoglycoside-induced and nonsyndromic hearing loss.** *Mitochondrion* 2010, **10**:380-390.
28. Konings A, Van Camp G, Goethals A, Van Eyken E, Vandevelde A, Ben Azza J, Peeters N, Wuyts W, Smeets H, Van Laer L: **Mutation analysis of mitochondrial DNA 12SrRNA and tRNASer(UCN) genes in non-syndromic hearing loss patients.** *Mitochondrion* 2008, **8**:377-382.
29. Kobayashi K, Oguchi T, Asamura K, Miyagawa M, Horai S, Abe S, Usami S: **Genetic features, clinical phenotypes, and prevalence of sensorineural hearing loss associated with the 961delT mitochondrial mutation.** *Auris Nasus Larynx* 2005, **32**:119-124.
30. Yao YG, Salas A, Bravi CM, Bandelt HJ: **A reappraisal of complete mtDNA variation in East Asian families with hearing impairment.** *Hum Genet* 2006, **119**:505-515.
31. Herrnstadt C, Howell N: **An evolutionary perspective on pathogenic mtDNA mutations: haplogroup associations of clinical disorders.** *Mitochondrion* 2004, **4**:791-798.
32. Kong QP, Bandelt HJ, Sun C, Yao YG, Salas A, Achilli A, Wang CY, Zhong L, Zhu CL, Wu SF, *et al*: **Updating the East Asian mtDNA phylogeny: a prerequisite for the identification of pathogenic mutations.** *Hum Mol Genet* 2006, **15**:2076-2086.
33. Tanaka M, Cabrera VM, Gonzalez AM, Larruga JM, Takeyasu T, Fuku N, Guo LJ, Hirose R, Fujita Y, Kurata M, *et al*: **Mitochondrial genome variation in eastern Asia and the peopling of Japan.** *Genome Res* 2004, **14**:1832-1850.
34. Achilli A, Perego UA, Bravi CM, Coble MD, Kong QP, Woodward SR, Salas A, Torroni A, Bandelt HJ: **The phylogeny of the four pan-American MtDNA haplogroups: implications for evolutionary and disease studies.** *PLoS One* 2008, **3**:e1764.
35. Usami S, Abe S, Akita J, Namba A, Shinkawa H, Ishii M, Iwasaki S, Hoshino T, Ito J, Doi K, *et al*: **Prevalence of mitochondrial gene mutations among hearing impaired patients.** *J Med Genet* 2000, **37**:38-40.
36. Oshima T, Kudo T, Ikeda K: **Point mutation of the mitochondrial genome in Japanese deaf-mutism.** *ORL J Otorhinolaryngol Relat Spec* 2001, **63**:329-332.
37. He Y, Wu J, Dressman DC, Iacobuzio-Donahue C, Markowitz SD, Velculescu VE, Diaz LA Jr, Kinzler KW, Vogelstein B, Papadopoulos N: **Heteroplasmic mitochondrial DNA mutations in normal and tumour cells.** *Nature* 2010, **464**:610-614.
38. Lu J, Wang D, Li R, Li W, Ji J, Zhao J, Ye W, Yang L, Qian Y, Zhu Y, *et al*: **Maternally transmitted diabetes mellitus associated with the mitochondrial tRNA(Leu(UUR)) A3243G mutation in a four-generation Han Chinese family.** *Biochem Biophys Res Commun* 2006, **348**:115-119.
39. Mancuso M, Filosto M, Forli F, Rocchi A, Berrettini S, Siciliano G, Murri L: **A non-syndromic hearing loss caused by very low levels of the mtDNA A3243G mutation.** *Acta Neurol Scand* 2004, **110**:72-74.
40. Laloi-Michelin M, Meas T, Ambonville C, Bellanne-Chantelot C, Beaufils S, Massin P, Vialettes B, Gin H, Timsit J, Bauduceau B, *et al*: **The clinical variability of maternally inherited diabetes and deafness is associated with the degree of heteroplasmy in blood leukocytes.** *J Clin Endocrinol Metab* 2009, **94**:3025-3030.
41. van Den Bosch BJ, de Coo RF, Scholte HR, Nijland JG, van Den Bogaard R, de Visser M, de Die-Smulders CE, Smeets HJ: **Mutation analysis of the entire mitochondrial genome using denaturing high performance liquid chromatography.** *Nucleic Acids Res* 2000, **28**:E89.
42. Matsunaga T, Hirota E, Bito S, Niimi S, Usami S: **Clinical course of hearing and language development in GJB2 and non-GJB2 deafness following habilitation with hearing aids.** *Audiol Neurootol* 2006, **11**:59-68.
43. Matsunaga T, Kumanomido H, Shiroma M, Ohtsuka A, Asamura K, Usami S: **Deafness due to A1555G mitochondrial mutation without use of aminoglycoside.** *Laryngoscope* 2004, **114**:1085-1091.
44. Wada Y, Kayamori Y, Hamasaki N: **Protocols for entire mitochondrial DNA sequence by direct sequencing.** *Rinsho-Kensa* 2005, **49**:59-64, (Japanese).
45. **Hereditary Hearing Loss Homepage.** [http://hereditaryhearingloss.org/].
46. Anderson S, Bankier AT, Barrell BG, de Bruijn MH, Coulson AR, Drouin J, Eperon IC, Nierlich DP, Roe BA, Sanger F, *et al*: **Sequence and organization of the human mitochondrial genome.** *Nature* 1981, **290**:457-465.
47. Andrews RM, Kubacka I, Chinnery PF, Lightowlers RN, Turnbull DM, Howell N: **Reanalysis and revision of the Cambridge reference sequence for human mitochondrial DNA.** *Nat Genet* 1999, **23**:147.
48. **mtSNP database.** [http://mtsnp.tmig.or.jp/mtsnp/index.shtml].
49. **MITOMAP.** [http://www.mitomap.org/MITOMAP].
50. **Uppsala mtDB database.** [http://www.genpat.uu.se/mtDB/].
51. Leveque M, Marlin S, Jonard L, Procaccio V, Reynier P, Amati-Bonneau P, Baulande S, Pierron D, Lacombe D, Duriez F, *et al*: **Whole mitochondrial genome screening in maternally inherited non-syndromic hearing impairment using a microarray resequencing mitochondrial DNA chip.** *Eur J Hum Genet* 2007, **15**:1145-1155.
52. **PhyloTree.** [http://www.phylotree.org/].
53. Hamada M, Kiryu H, Sato K, Mituyama T, Asai K: **Prediction of RNA secondary structure using generalized centroid estimators.** *Bioinformatics* 2009, **25**:465-473.
54. Sato K, Hamada M, Asai K, Mituyama T: **CENTROIDFOLD: a web server for RNA secondary structure prediction.** *Nucleic Acids Res* 2009, **37**:W277-280.
55. Mollers M, Maniura-Weber K, Kiseljakovic E, Bust M, Hayrapetyan A, Jaksch M, Helm M, Wiesner RJ, von Kleist-Retzow JC: **A new mechanism for mtDNA pathogenesis: impairment of post-transcriptional maturation leads to severe depletion of mitochondrial tRNASer(UCN) caused by T7512C and G7497A point mutations.** *Nucleic Acids Res* 2005, **33**:5647-5658.
56. Tang X, Yang L, Zhu Y, Liao Z, Wang J, Qian Y, Tao Z, Hu L, Wu G, Lan J, *et al*: **Very low penetrance of hearing loss in seven Han Chinese pedigrees carrying the deafness-associated 12S rRNA A1555G mutation.** *Gene* 2007, **393**:11-19.
57. Torroni A, Campos Y, Rengo C, Sellitto D, Achilli A, Magri C, Semino O, Garcia A, Jara P, Arenas J, *et al*: **Mitochondrial DNA haplogroups do not play a role in the variable phenotypic presentation of the A3243G mutation.** *Am J Hum Genet* 2003, **72**:1005-1012.
58. Takahashi K, Merchant SN, Miyazawa T, Yamaguchi T, McKenna MJ, Kouda H, Iino Y, Someya T, Tamagawa Y, Takiyama Y, *et al*: **Temporal bone histopathological and quantitative analysis of mitochondrial DNA in MELAS.** *Laryngoscope* 2003, **113**:1362-1368.

59. Tiranti V, Chariot P, Carella F, Toscano A, Soliveri P, Girlanda P, Carrara F, Fratta GM, Reid FM, Mariotti C, *et al*: **Maternally inherited hearing loss, ataxia and myoclonus associated with a novel point mutation in mitochondrial tRNASer(UCN) gene.** *Hum Mol Genet* 1995, **4**:1421-1427.
60. Tang X, Li R, Zheng J, Cai Q, Zhang T, Gong S, Zheng W, He X, Zhu Y, Xue L, *et al*: **Maternally inherited hearing loss is associated with the novel mitochondrial tRNA Ser(UCN) 7505T > C mutation in a Han Chinese family.** *Mol Genet Metab* 2010, **100**:57-64.
61. Sue CM, Tanji K, Hadjigeorgiou G, Andreu AL, Nishino I, Krishna S, Bruno C, Hirano M, Shanske S, Bonilla E, *et al*: **Maternally inherited hearing loss in a large kindred with a novel T7511C mutation in the mitochondrial DNA tRNA(Ser(UCN)) gene.** *Neurology* 1999, **52**:1905-1908.
62. Young WY, Zhao L, Qian Y, Wang Q, Li N, Greinwald JH Jr, Guan MX: **Extremely low penetrance of hearing loss in four Chinese families with the mitochondrial 12S rRNA A1555G mutation.** *Biochem Biophys Res Commun* 2005, **328**:1244-1251.
63. Rydzanicz M, Wrobel M, Cywinska K, Froehlich D, Gawecki W, Szyfter W, Szyfter K: **Screening of the general Polish population for deafness-associated mutations in mitochondrial 12S rRNA and tRNA Ser(UCN) genes.** *Genet Test Mol Biomarkers* 2009, **13**:167-172.

**Pre-publication history**

The pre-publication history for this paper can be accessed here:
http://www.biomedcentral.com/1471-2350/12/135/prepub

doi:10.1186/1471-2350-12-135
**Cite this article as:** Mutai *et al.*: Systematic analysis of mitochondrial genes associated with hearing loss in the Japanese population: dHPLC reveals a new candidate mutation. *BMC Medical Genetics* 2011 **12**:135.

*Acta Oto-Laryngologica*, 2011; 131: 1232–1236

informa
healthcare

SHORT COMMUNICATION

# Different cortical metabolic activation by visual stimuli possibly due to different time courses of hearing loss in patients with *GJB2* and *SLC26A4* mutations

HIDEAKI MOTEKI[1], YASUSHI NAITO[2], KEIZO FUJIWARA[2], RYOSUKE KITOH[1], SHIN-YA NISHIO[1], KAZUHIRO OGUCHI[3], YUTAKA TAKUMI[1] & SHIN-ICHI USAMI[1]

[1]*Department of Otorhinolaryngology, Shinshu University School of Medicine, Matsumoto,* [2]*Department of Otorhinolaryngology, Kobe City Medical Center General Hospital, Kobe and* [3]*Positron Imaging Center, Aizawa Hospital, Matsumoto, Japan*



**Abstract**

*Conclusion.* We have demonstrated differences in cortical activation with language-related visual stimuli in patients who were profoundly deafened due to genetic mutations in *GJB2* and *SLC26A4*. The differences in cortical processing patterns between these two cases may have been influenced by the differing clinical courses and pathogenesis of hearing loss due to genetic mutations. Our results suggest the importance of hearing during early childhood for the development of a normal cortical language network. *Objectives.* To investigate the cortical activation with language-related visual stimuli in patients who were profoundly deafened due to genetic mutations in *GJB2* and *SLC26A4*. *Methods:* The cortical activity of two adult patients with known genetic mutations (*GJB2, SLC26A4*) was evaluated with fluorodeoxyglucose-positron emission tomography (FDG-PET) with a visual language task and compared with that of normal-hearing controls. *Results:* A patient with a *GJB2* mutation showed activation in the right auditory association area [BA21, BA22], and the left auditory association area [BA42] even with visual language task; in contrast, a patient with an *SLC26A4* mutation showed no significant activation in the corresponding area.

**Keywords:** *FDG-PET, visual language task, functional brain imaging*

## Introduction

Functional brain imaging is an effective method for investigating the cortical processing of language, which has provided much evidence for the plasticity of the central auditory pathway following a profound loss of hearing [1–4]. Many previous studies showed that there is a capacity of the auditory cortex for cross-modal plasticity after auditory deprivation of the brain. Cerebral glucose metabolism in the primary auditory and related cortices in individuals with prelingual deafness was shown to decrease in younger patients, but to increase as they aged and, in fact, recover fully or even exceed the normal level of activation [5–7]. Children with prelingual deafness can acquire spoken language by cochlear implantation, but its efficacy decreases with age. The development of the auditory cortex is believed to depend on the patient's auditory experience within 'critical periods' in the early lifetime. Adults who had severe congenital hearing loss in their childhood may take advantage of hearing with cochlear implants if they had exploited residual hearing with hearing aids. It has been shown that low glucose metabolism in the temporal auditory cortex predicts a good cochlear implant outcome in prelingually deafened children, which suggests that low metabolism in the auditory cortex may indicate its potential of plasticity for spoken language acquisition [7].

Correspondence: Shin-ichi Usami, MD PhD, Department of Otorhinolaryngology, Shinshu University School of Medicine, 3-1-1 Asahi, Matsumoto 390-8621, Japan. Tel: +81 263 37 2666. Fax: +81 263 36 9164. E-mail: usami@shinshu-u.ac.jp

*(Received 9 March 2011; accepted 29 May 2011)*

ISSN 0001-6489 print/ISSN 1651-2251 online 
DOI: 10.3109/00016489.2011.593719

Meanwhile, several etiological studies suggest that at least 60% of congenital hearing loss has genetic causes. Recent advances in molecular genetics have made genetic diagnosis possible [8]. The identification of the mutation responsible for hearing loss may provide some information as to cochlear damage, and help predict the time course and manifestations of hearing loss. Genetic testing can therefore be useful in decision-making regarding cochlear implantation and other necessary treatment.

Evaluation of brain function and diagnosing accurate etiology of hearing loss may be the keys to personalizing post-cochlear implantation habilitation programs and predicting the outcomes thereof.

In this study, we used 18 F-fluorodeoxyglucose (FDG) positron emission tomography (PET) to measure cortical glucose metabolism with a visual language task before cochlear implantation in profoundly deaf patients whose etiologies were identified by genetic testing.



## Material and methods

### *Genetic diagnosis*

Genetic screening was performed in two cases using an Invader assay to screen for 41 known hearing loss-related mutations [9] and direct sequencing for *GJB2* and *SLC26A4* mutations [10,11].

### *FDG-PET scanning and image analysis*

FDG-PET scanning and image analysis were performed using the method described by Fujiwara et al. [12]. During the time period between the intravenous injection of 370 MBq 18 F-FDG (the dose was adjusted according to the body weight of each subject) and the PET scanning of the brain, the patients were instructed to watch a video of the face of a speaking person reading a children's book. The video lasted for 30 min, and several still illustrations taken from the book were inserted (for a few seconds each) to help the subjects to follow the story. The subjects were video-recorded to confirm that they were watching the task video. PET images were acquired with a GE ADVANCE NXi system (General Electric Medical Systems, Milwaukee, WI, USA). Spatial preprocessing and statistical analysis were performed with SPM2 (Institute of Neurology, University College of London, UK) implemented in Matlab (Mathworks, MA, USA). The cortical radioactivity of each deaf patient was compared with that of a control group of normal-hearing adults by a $t$ test in the basic model of SPM2. The statistical significance level was set at $p < 0.001$ (uncorrected).

This study was approved by the Ethics Committee of Shinshu University School of Medicine and written consent was obtained from each participant.

### *Control group*

The control group consisted of six normal-hearing right-handed adult subjects. The average (mean ± standard deviation) age of the normal-hearing subjects was 27.5 ± 3.8 years. The pure-tone average hearing levels were within 20 dB HL for all.

### *Case 1*

A right-handed 22-year-old female with a *GJB2* mutation (235 delC homozygous) had hearing impairment that was noticed by her parents when she was 2 years old. She had used hearing aids ever since, but with insufficient hearing amplification. She used lip-reading and some sign language, and her speech was not intelligible to hearing people. Computed tomography (CT) findings of the middle and inner ear were normal. Her average pure-tone hearing levels were 102.5 dB for the right ear and 95 dB for the left ear (Figure 1A).

### *Case 2*

A right-handed 26-year-old male with an *SLC26A4* mutation (H723R homozygous) had hearing impairment that was noticed by his parents when he was 2 years old, from which time he had used hearing aids bilaterally. He did not use lip-reading or sign language during the acquisition age for language. He obtained spoken language with hearing aids but had progressive hearing loss, and sometimes suffered vertigo attacks. His pronunciation was clear, and his speech was almost completely intelligible. CT findings exhibited an enlarged vestibular aqueduct on each side. His average pure-tone hearing levels were 106.2 dB for the right ear and 100 dB for left ear (Figure 1B).

## Results

Figure 2 shows transaxial PET images of each participant's brain. The visual stimuli resulted in bilateral activation of the superior temporal gyrus, including Heschl's gyrus in case 1 with *GJB2* mutation (Figure 2A, white arrowhead). In contrast, in case 2 with *SLC26A4* mutation, the activation of the superior temporal gyrus was much lower than in case 1 (Figure 2B, white arrowhead).

Figure 3 shows supra-threshold clusters in each case. In case 1, activation higher than normal controls

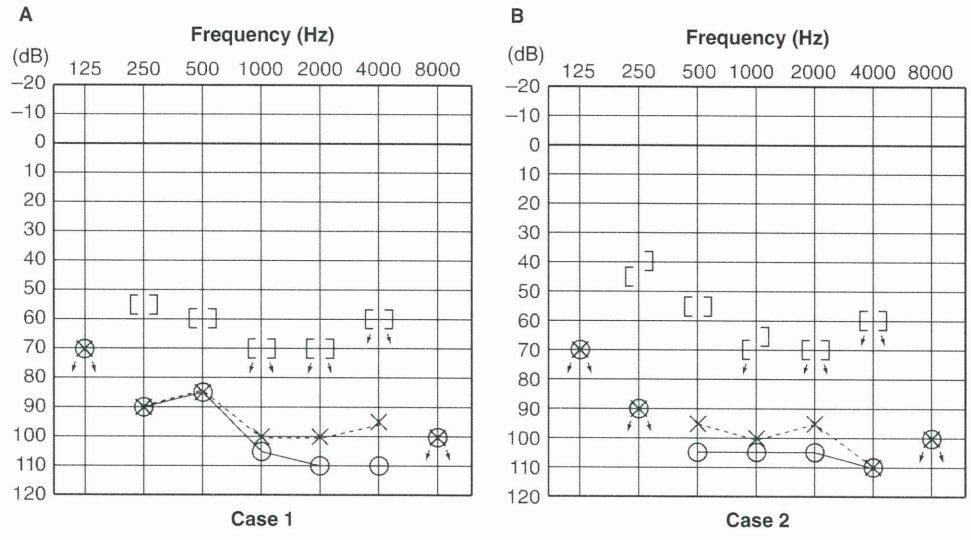


Figure 1. Pure-tone audiograms: (A) a 22-year-old female with a *GJB2* mutation; (B) a 26-year-old male with an *SLC26A4* mutation. There were no clear differences in hearing thresholds in these two cases.

was observed in the right auditory association area [BA21, BA22], and the left auditory association area [BA42] ($p < 0.001$). In case 2, the right superior frontal gyrus [BA9], and the middle temporal gyrus [BA20], showed higher activation than normal controls ($p < 0.001$).

## Discussion

More than half of congenital hearing loss has been estimated to be from genetic causes, and phenotypes are affected by genetic mutations. There have been no reports of the influence of phenotype on brain function associated with hearing. This is the first report on evaluation of cortical processing of language in patients with genetic mutations as a main etiology of hearing loss. The auditory association area was activated bilaterally in case 1 (*GJB2* mutation), but not activated in case 2 (*SLC26A4* mutation). A previous study indicated that the temporal lobe is activated during speech-reading in normal subjects [13] and another study found that the temporal lobe is not activated when reading fluent speech from a talking face [14]. For the present study we used a

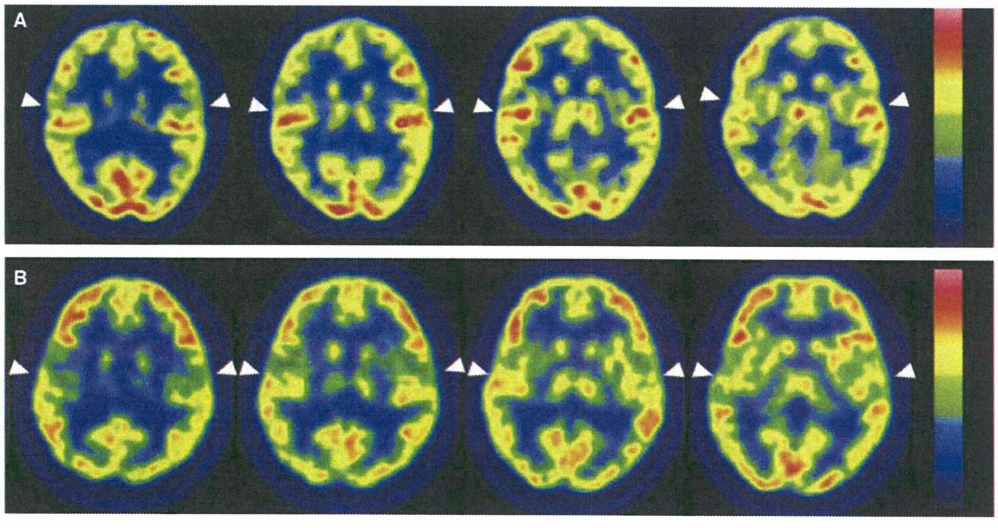


Figure 2. Transaxial PET images of each participant's brain: activation (arrowheads) of the superior temporal gyrus with visual language stimuli in each case. (A) Case 1 (*GJB2* mutation). The superior temporal gyri were strongly activated bilaterally. (B) Case 2 (*SLC26A4* mutation). The superior temporal gyri exhibited less activation than in case 1.

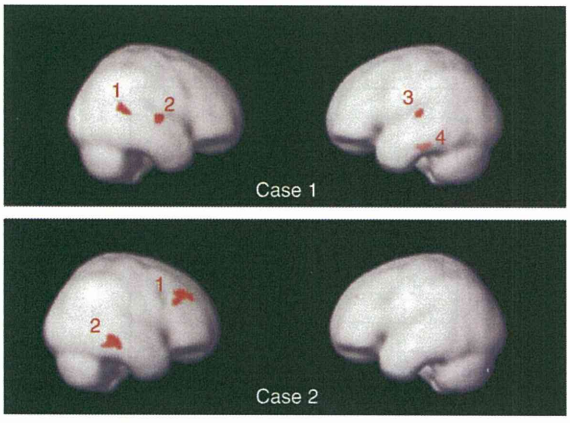


Figure 3. Cortical activation by language-related visual stimuli in the two profoundly deafened cases. Case 1 (*GJB2* mutation) showed significant activation in the right middle temporal gyrus [BA21] (1), superior temporal gyrus [BA22] (2), and left superior temporal gyrus [BA42] (3), and left cerebellum (4), while case 2 (*SLC26A4* mutation) exhibited significant activation in the right superior frontal gyrus [BA9] (1), and middle temporal gyrus [BA20] (2) (SPM2, $p < 0.001$, uncorrected).

fluent speech-reading task, similar to that described by Hall et al. [14]. Fujiwara et al. in a FDG-PET study using the same methods and task as the present study, showed that subjects with better spoken language skills had less temporal lobe activation [12].

To summarize these reports, the patients with hearing aids with better spoken language skills have less temporal lobe activation with a visual language task. Otherwise, Nishimura et al. [15] reported a sign language activation of the bilateral auditory association areas in a congenitally deafened subject. However, detailed clinical data for the subject – including his hearing levels, time course of hearing loss, and the cause of deafness – were not described. The different visual language activation patterns in the auditory cortices revealed in the current two profoundly deafened subjects with different genetic etiologies and hearing loss progressions may, thus, add further knowledge of the cross-modal plasticity brought about in the superior temporal association areas by lack of hearing.

The differences in cortical processing patterns between cases 1 and 2 – who both had hearing loss of cochlear origin – may have been influenced by the differing clinical courses of hearing loss. *GJB2* is currently known to be the most prevalent gene responsible for congenital hearing loss worldwide. Patients with severe phenotypes who have *GJB2* mutations are good candidates for implantation, because their hearing loss is of cochlear origin and non-progressive [16,17]. *SLC26A4* is known as a commonly found gene and is associated with enlarged vestibular aquaduct [11]. This phenotype includes congenital and progressive hearing loss, usually associated with vertigo [18]. In most cases hearing remains in low frequencies, enabling the understanding of spoken language with hearing aids. Cochlear implantation has resulted in remarkable improvements in auditory skills and speech perception for patients with profound hearing loss associated with *SLC26A4* mutations as well as *GJB2*.

Comparing case 1 (*GJB2* mutation) with case 2 (*SLC26A4* mutation), the crucial importance of the use of hearing aids during childhood up to age 6 years for acquisition of better hearing is evident. In case 1, even though she was able to hear sound with the use of hearing aids, she was unable to recognize enough speech language due to insufficient hearing amplification during the critical periods in her childhood. She therefore used lip-reading and some sign language in addition to hearing aids. Increased metabolism was observed by FDG-PET in the auditory association area, where no significant activation was found in the normal-hearing controls. In contrast, in case 2, a 26-year-old patient with an *SLC26A4* mutation, there was no significant activation in the corresponding area. He obtained rather hearing ability and spoken language by hearing aids with residual hearing at lower frequencies during his childhood. His hearing was supposed to be better than case 1, because 1) he did not use lip-reading or sign language during the acquisition age for language from anamnestic evaluation; 2) his pronunciation was clear, indicating better hearing (at least 40–50 dB) during the acquisition age for language; 3) from an etiological point of view, patients with *SLC26A4* mutation usually have mild to moderate hearing loss during childhood and this shows a progressive nature [18]. He had progressive hearing loss in the natural history as a phenotype of *SLC26A4* mutation. The difference in activation patterns in the cases with *GJB2* and *SLC26A4* mutations was clearly demonstrated by statistical processing with SPM, as well as in the PET scans. These results suggest the importance of hearing during early childhood for the development of a normal cortical language network, and that reorganization had occurred in the auditory cortex of the patient with a *GJB2* mutation; i.e. processing visual aspects of language in the superior temporal gyri. This implies that cross-modal plasticity as a consequence of the lack of hearing during the critical period for spoken language acquisition in early childhood was influenced by the time course of hearing loss characterized by genetic mutations.

Previous studies have suggested that auditory areas presented high accumulation of FDG with deafness of early onset, and plastic changes in auditory cortices